Eur. J. Phycol., (2006), **41(3)**: 337–362

Taylor & Francis
Taylor & Francis Group

Phylogeny and taxonomy of *Halimeda incrassata*, including descriptions of *H. kanaloana* and *H. heteromorpha* spp. nov. (Bryopsidales, Chlorophyta)

HEROEN VERBRUGGEN[1], OLIVIER DE CLERCK[1], ANTOINE D.R. N'YEURT[2], HEATHER SPALDING[3] AND PETER S. VROOM[4]

[1]*Phycology Research Group & Centre for Molecular Phylogenetics and Evolution, Ghent University, Krijgslaan 281 (S8), B-9000, Gent, Belgium*
[2]*Laboratoire Terre-Ocean (Ecologie Marine), Université de la Polynésie française, B.P. 6570, Faa'a, Tahiti 98702, French Polynesia*
[3]*Botany Department, University of Hawai'i at Manoa, 3190 Maile Way, Honolulu, Hawai'i 96822, USA*
[4]*Joint Institute for Marine and Atmospheric Research, Research Corporation of the University of Hawai'i, contracted to the Coral Reef Ecosystem Division (CRED), Pacific Islands Fisheries Science Center, NOAA Fisheries and Ecosystems, 1125B Ala Moana Boulevard, Honolulu, Hawai'i 96814, USA*

(Received 10 February 2005; accepted 7 March 2006)

The tropical green algal genus *Halimeda* is one of the best studied examples of pseudo-cryptic diversity within the algae. Previous molecular and morphometric studies revealed that within *Halimeda* section *Rhipsalis*, *Halimeda incrassata* included three pseudo-cryptic entities and that the morphological boundaries between *H. incrassata* and *Halimeda melanesica* were ill-defined. In this paper, the taxonomy of *H. incrassata* is revised: two pseudo-cryptic entities are described as new species, *Halimeda kanaloana* and *Halimed heteromorpha*, while *H. incrassata* is redefined to encompass a single, monophyletic entity. Similarities and differences between the three species and *H. melanesica* are discussed. Monophyly of *H. heteromorpha*, which was questioned in a former study, is reinvestigated using sets of 32 ITS1–ITS2 and 21 plastid *rps*3 sequences and various alignment and inference methods. The phylogenetic relationships within *Halimeda* section *Rhipsalis* are inferred from nuclear 18S–ITS1–5.8S–ITS2 and concatenated plastid sequences (*tuf*A & *rpl*5–*rps*8–*inf*A) and interpreted in a biogeographic context.

Key words: anatomy, *Halimeda incrassata*, *H. heteromorpha*, *H. kanaloana*, *H. melanesica*, morphology, phylogeny, taxonomy

Introduction

Marine macroalgae of the chlorophyte genus *Halimeda* Lamouroux abound throughout the tropics and are easily recognized by their green, calcified segments. They are ecologically important reef algae throughout the tropical Indo-Pacific and Caribbean Sea, being prominent primary producers (Littler *et al.*, 1988), sources of food and habitat (e.g. Rossier & Kulbicki, 2000; Chittaro, 2004) and carbonate sand producers (e.g. Drew, 1983; Freile *et al.*, 1995; Payri, 1995).

Halimeda is divided into five sections based on molecular, ecological and morphological features (Kooistra *et al.*, 2002; Verbruggen & Kooistra, 2004). Taxonomic problems in speciose sections are obvious. Some species boundaries are ambiguously defined (Verbruggen *et al.*, 2005*a*), and several cases of cryptic and pseudo-cryptic diversity are known (Kooistra *et al.*, 2002; Verbruggen *et al.*, 2005*a*, *b*). DNA barcoding and morphometric analyses are being used to repartition the genus into genetically and morphologically distinct species (Kooistra & Verbruggen, 2005; Verbruggen *et al.*, 2005*a*, *b*).

Halimeda section *Rhipsalis* J. Agardh ex De Toni is characterized by pores that interconnect medullar siphons at nodes, and segment agglutination in the basal thallus region (Verbruggen & Kooistra, 2004). It contains 11 tropical species, four of which are restricted to the Atlantic Ocean, and seven of which are Indo-Pacific (Verbruggen *et al.*, 2005*a*). Even though most species extend throughout the Caribbean or the Indo-Pacific, some have very restricted distribution ranges. For instance, *Halimeda stuposa* Taylor and *Halimeda favulosa*

Correspondence to: Heroen Verbruggen. e-mail: heroen.verbruggen@ugent.be

ISSN 0967-0262 print/ISSN 1469-4433 online/06/030337–26 © 2006 British Phycological Society
DOI: 10.1080/09670260600709315

Howe seem to be endemic to the Marshall Islands and the Bahamas, respectively.

The section was recently studied using both molecular and morphometric techniques (Verbruggen *et al*., 2005*a*). This allowed redefinition of formerly ill-defined species within the following morphological groups: *Halimeda borneensis* Taylor – *Halimeda simulans* Howe and *Halimeda cylindracea* Decaisne – *Halimeda monile* (Ellis & Solander) Lamouroux. *Halimeda incrassata* (Ellis) Lamouroux was shown to comprise three pseudo-cryptic entities, initially recognized by deviant DNA sequences and subsequently characterized using morphometric techniques (Kooistra *et al*., 2002; Verbruggen *et al*., 2005*a*). Noble (1987) noted that the species boundary between *Halimeda melanesica* Valet and *H. incrassata* was blurred because the absence of nodal fusions, diagnostic for *H. melanesica*, is not constant within the species. Verbruggen *et al*. (2005*a*) corroborated this but showed that *H. melanesica* and *H. incrassata* are genetically distinct and that other morphological characters allow distinction between the entities.

The putative paraphyly of *H. incrassata* 1a, a pseudo-cryptic species within *H. incrassata* (Verbruggen *et al*., 2005*a*) is also interesting. This species, described below as *Halimeda heteromorpha* sp. nov., was monophyletic in a maximum parsimony (MP) phylogram inferred from *rps*3 sequences. However, in a MP phylogram of ITS1–5.8S–ITS2 sequences, *H. incrassata* 1b (described below as *Halimeda kanaloana* sp. nov.) branched off within *H. incrassata* 1a, leaving the latter paraphyletic.

This paper revises *H. incrassata* by describing and comparing the morphology, distribution and ecology of its pseudo-cryptic component species. The species are also compared with *H. melanesica*. The monophyly of *H. incrassata* 1a (*H. heteromorpha*) is investigated in more detail, by exploring the evolutionary relationships between large sets of sequences of *Halimeda macroloba* Decaisne, *H. heteromorpha* and *H. kanaloana* using multiple inference methods and alternative sequence alignments. The evolutionary and biogeographic history of *Halimeda* section *Rhipsalis* is also explored by phylogenetic analysis of plastid and nuclear DNA sequence data.

Materials and methods

Taxa from *Halimeda* section *Rhipsalis* were collected throughout most of their distribution ranges. Specimens were preserved in 95% ethanol or silica-gel for molecular analyses and in wet preservative (95% ethanol or 5% formalin) for anatomical observations.

Observations and measurements of vegetative and reproductive structures were carried out as in Vroom & Smith (2003) and Verbruggen *et al*. (2005*a*, *c*). Specimens were identified using the key of Verbruggen *et al*. (2005*a*). Geographic origins and herbarium accession numbers of examined specimens are listed in the Appendix. Extraction of DNA followed Kooistra *et al*. (2002).

To investigate evolutionary relationships within the section, three DNA sequence sets were created. Two plastid DNA (cpDNA) regions (partial *tuf*A, *rpl*5–*rps*8–*inf*A region) and the nuclear ribosomal cistron (nrDNA: 18S [SSU] from around position 500, ITS1, 5.8S, ITS2, and about 50 bases into 28S [LSU]) were amplified according to Famà *et al*. (2002), Provan *et al*. (2004), and Kooistra *et al*. (2002) respectively. Amplified products were sequenced with an ABI Prism 3100 automated sequencer (Applied Biosystems, Foster City, CA) and submitted to Genbank (Appendix). For the plastid regions, *Halimeda gracilis* Harvey *ex* J. Agardh, *Halimeda taenicola* Taylor, *Halimeda opuntia* (Linneaus) Lamouroux and *Halimeda micronesica* Yamada were sequenced as close outgroups and *Avrainvillea rawsonii* (Dickie) Howe, *Pseudocodium floridanum* Dawes & Mathieson, *Tydemania expeditionis* Weber van Bosse and *Udotea orientalis* Gepp & Gepp as more distant outgroups (Appendix). Sequences from the nuclear 18S–ITS1–5.8S–ITS2 region of ingroup taxa, as well as *Halimeda discoidea* Decaisne, *H. micronesica*, *H. gracilis* and *H. opuntia* as close outgroup taxa and *Udotea flabellum* (Ellis & Solander) Howe, *Penicillus capitatus* Lamarck and *Flabellia petiolata* (Turra) Nizamuddin as more distant outgroups were downloaded from GenBank (accession numbers listed in Appendix). Partial *tuf*A and *rpl*5–*rps*8–*inf*A sequences were aligned with ClustalW 1.82 as described in Verbruggen *et al*. (2005*b*). The *tuf*A and *rpl*5–*rps*8–*inf*A sequence data sets were concatenated before analysis. The 18S–ITS1–5.8S–ITS2 sequences were aligned by eye, starting from the alignment of Verbruggen & Kooistra (2004). All alignments used in this study are available from the corresponding author upon request.

Nuclear and plastid DNA data sets were subjected to maximum likelihood (ML) analysis in PAUP* 4.0b10 (Swofford, 2003), using the nucleotide substitution model suggested by hierarchical likelihood ratio tests (hLRT) implemented in Modeltest 3.5 (Posada & Crandall, 1998). Starting trees were obtained by stepwise random sequence addition. A single tree was retained at each step. Branch swapping was achieved by tree bisection-reconnection (TBR). The number of rearrangements was limited to 1,000 per addition-sequence replicate. The analysis was performed with 25 addition-sequence replicates. ML bootstrapping (100 replicates) was performed with the same settings. MP bootstrapping (100 replicates) was performed with 100 addition-sequence replicates per bootstrap replicate, limiting the number of rearrangements per addition-sequence replicate to 100 million, and treating gaps as missing data.

To reinvestigate the monophyly of *H. heteromorpha*, two batches of sequences were downloaded from

Genbank (Appendix). The first batch of sequences consisted of 32 18S–ITS1–5.8S–ITS2–28S sequences of *H. macroloba* (11 sequences), *H. heteromorpha* (= *H. incrassata* 1a; 16 sequences), and *H. kanaloana* (= *H. incrassata* 1b; 5 sequences). Two alignments were created from this batch of sequences: (i) the ClustalW alignment used in Verbruggen *et al.* (2005*a*), and (ii) a manual gap block coding alignment. In the latter alignment, which is a variant of block coding (Geiger, 2002), individual bases and sequence blocks showing ambiguous alignment between species were separated and individual gaps or blocks of gaps were inserted for the species in which this base or sequence block was absent. Partial 18S, 5.8S and partial 28S were removed from both alignments because they were virtually invariant. The alignments were subjected to three inference methods (ML, MP and Bayesian Inference). ML analysis was carried out in PAUP* 4.0b10, using the nucleotide substitution model selected by hLRT in MrModeltest 2.0 (Nylander, 2004). Options for ML analysis were: starting trees by stepwise random sequence addition, retaining a single tree at each step, TBR branch swapping, maximum 1,000 rearrangements per addition-sequence replicate, 50 addition-sequence replicates. ML bootstrapping (100 replicates) was carried out with five addition-sequence replicates per bootstrap replicate. MP analysis was carried out in PAUP* 4.0b10, with the following options: starting trees by stepwise random sequence addition, retaining multiple trees at each step, TBR branch swapping, maximum 10^8 rearrangements per addition-sequence replicate, 100 addition-sequence replicates, with gaps treated as fifth base. MP bootstrapping (100 replicates) was carried out with the same settings. Bayesian inference (BI) was performed in MrBayes 3.0B4 (Ronquist & Huelsenbeck, 2003), using the nucleotide substitution model selected by MrModeltest 2.0. Analyses were run with four Markov chains for 10^6 generations, with a tree saved every 100^{th} generation. The first 1,000 trees were discarded as burn-in. Eleven *H. macroloba* sequences were used as outgroups for ML and MP analysis; one of these (AF525562) was used for BI.

The second batch of sequences downloaded for the reinvestigation of *H. heteromorpha* monophyly consisted of 21 plastid *rps*3 sequences of *H. incrassata* 2, *H. monile*, *H. simulans*, *H. melanesica*, *H. borneensis*, *H. macroloba* (one sequence of each), *H. heteromorpha* (= *H. incrassata* 1a; 11 sequences) and *H. kanaloana* (= *H. incrassata* 1b; four sequences). These protein-coding sequences were aligned on the basis of a blueprint created by ClustalW 1.82 alignment of their amino acid sequences. ML, MP and BI analyses were carried out as detailed above for the ITS1–ITS2 sequence alignments. Sequences of *H. simulans*, *H. incrassata* 2, *H. monile*, *H. borneensis* and *H. melanesica* were used as outgroups for ML and MP analyses; the *H. incrassata* 2 sequence was used for BI.

Herbarium acronyms are as follows: BISH: Bishop Museum, Honolulu, Hawai'i, USA; GENT: Ghent University Herbarium, Ghent, Belgium; L: National Herbarium of the Netherlands, Leiden University branch, Leiden, The Netherlands; PC: Muséum National d'Histoire Naturelle, Paris, France; UPF: University of French Polynesia Herbarium, Tahiti, French Polynesia; US: US National Herbarium, Smithsonian Institution, Washington DC, USA.

Results and discussion

Phylogeny and biogeography of section Rhipsalis

Sequences from the nuclear ribosomal DNA cistron included part of the 18S gene (from around position 500), the ITS1–5.8S–ITS2 region, and about 50 bases of the 28S gene, totalling between 1,724 and 1,755 bases in length. The relatively conserved 18S, 5.8S and 28S sequences could be readily aligned with very few gap introductions. Within the ITS regions, variable and conserved parts alternated. Alignment of the more variable parts required the introduction of gaps. Of 1,840 aligned positions, 247 were parsimony informative. The Modeltest hLRT selected the four-parameter Tamura and Nei (1993) substitution model with substitution rates varying over sites according to a gamma distribution (shape = 0.5151) and the proportion of invariable sites equal to 0.5824.

Partial *tuf*A sequences were of equal length (859 base pairs) without indels. There was a wide range in lengths of the *rpl*5–*rps*8–*inf*A region (686–808 base pairs) due to large differences in the *rps*8–*inf*A spacer, which was excluded from analyses. Coding regions were almost constant in length and aligned readily. Two codon gaps were introduced to align the ingroup sequences; inclusion of outgroup sequences required several more codon gaps. Base substitutions in the *tuf*A and *rpl*5–*rps*8–*inf*A sequences occurred mainly at third codon positions. The concatenated alignment provided 1,600 positions, of which 359 were parsimony informative. The Modeltest hLRT again selected a Tamura and Nei (1993) substitution model, with rate variation across sites following a gamma distribution (shape = 0.3558).

Phylograms inferred from nrDNA and concatenated cpDNA sequences are shown in Figs 1 and 2, respectively. *Halimeda heteromorpha* and *H. kanaloana* correspond to the species denoted *H. incrassata* 1a and *H. incrassata* 1b, respectively, in Verbruggen *et al.* (2005*a*). We could not obtain suitable specimens for DNA extraction of two species of section *Rhipsalis* (*H. favulosa* and *H. stuposa*). Based on SSU nrDNA, Kooistra *et al.* (2002) showed that *H. stuposa* was closely related to *H. borneensis*, to the extent that the former was considered to be a stunted form of the latter. *Halimeda favulosa*, a rare species that is endemic to the Bahamas (Taylor, 1960; Hillis-Colinvaux, 1980), is presumed

to be closely related to the remaining Atlantic species *H. monile*, *H. simulans* and *H. incrassata*.

The nuclear phylogram (Fig. 1) contained two major lineages. The first clade contained the three Atlantic species; the second contained all Indo-Pacific species, within which all species except *H. cylindracea* formed a very well supported subgroup. The latter featured three lineages (*H. melanesica*, *H. borneensis* and the *H. macroloba–heteromorpha–kanaloana* lineage), between which the relationships are unresolved. The *H. heteromorpha–kanaloana* cluster received relatively high bootstrap support.

The cpDNA phylogram (Fig. 2) had a nearly identical topology, except that *H. melanesica* and *H. borneensis* formed a monophyletic group. The Indo-Pacific clade and its subgroup (excluding *H. cylindracea*) had moderate ML bootstrap support and less than 50% MP bootstrap support. Unlike in the nuclear tree, the *H. heteromorpha–kanaloana* cluster received low bootstrap support.

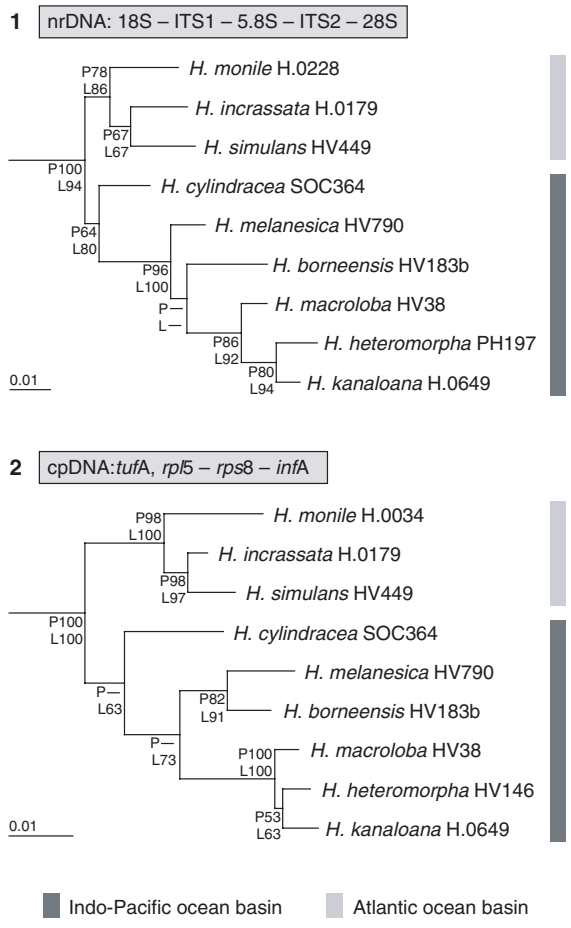

Figs 1–2. Phylograms inferred by maximum likelihood. Fig. 1. Phylogram inferred from SSU–ITS1–5.8S–ITS2 sequence data ($-\ln L = 6779.4578$). Fig. 2. Phylogram inferred from concatenated plastid sequence data ($-\ln L = 7600.43835$). Outgroups were pruned from the trees. Maximum parsimony (P) and maximum likelihood (L) bootstrap values are indicated at branches. Scale bars represent 0.01 substitutions per site. Grey bars along the right hand side indicate the geographic origin of species.

The clear-cut separation of Atlantic and Indo-Pacific species in the phylograms suggests separate diversification of *Halimeda* section *Rhipsalis* in the ocean basins. Previous research has shown basal or near-basal separation of Indo-Pacific and Atlantic species of all five sections of *Halimeda* (Kooistra *et al.*, 2002; Verbruggen & Kooistra, 2004; Verbruggen *et al.*, 2005*b*). This suggests that a vicariance event allowed independent diversification of the different sections in the Caribbean Sea and Indo-Pacific ocean basin (Kooistra *et al.*, 1999, 2002). This pattern is common in marine taxa of Tethyan origin, from parrotfishes (Streelman *et al.*, 2002) to mangrove trees (Ellison *et al.*, 1999). Closure of the Tethyan Seaway in the Middle East during the Miocene and the rise of the Central American Isthmus in the Pliocene are hypothesized vicariance events for *Halimeda* (Kooistra *et al.*, 1999, 2002; Verbruggen *et al.*, 2005*b*).

Evolution of the H. heteromorpha–kanaloana–macroloba *species cluster*

The plastid and nuclear phylograms (Figs 1, 2) exhibit a sister relationship between *H. kanaloana* and *H. heteromorpha*, although this relationship has only moderate bootstrap support in the cpDNA data set. More elaborate analyses with multiple specimens per species and different alignment methods shed more light on the evolution of the *H. heteromorpha–kanaloana–macroloba* species cluster.

After the ClustalW alignment of 18S–ITS1–5.8S–ITS2–28S sequences (Verbruggen *et al.*, 2005*a*) had been stripped of 18S, 5.8S, 28S sequences and all taxa except *H. macroloba*, *H. incrassata* 1a (= *H. heteromorpha*) and *H. incrassata* 1b (= *H. kanaloana*), 240 positions were aligned. ITS1 sequences were 78 to 89 bases long; ITS2 sequences were 141–146 bases long. The MrModeltest hLRT suggested a symmetrical model of base substitution (Zharkihk, 1994) with rate variation across sites (gamma shape parameter 0.3256) for the ITS1–ITS2 alignment.

The gap block coding alignment totalled 266 positions, 26 more than the ClustalW alignment. The MrModeltest hLRT suggested a Kimura (1980) base-substitution model with rate variation across sites (gamma shape parameter 0.2916).

Figures 3–8 show the 50% majority rule consensus trees for ML bootstrap, MP bootstrap, and BI analyses for both types of alignment of the ITS1–ITS2 data. All trees showed strong support for the clade containing *H. heteromorpha* and *H. kanaloana*, and *H. kanaloana* was monophyletic in all trees. However, the position of *H. kanaloana* relative to *H. heteromorpha* differed. In the MP and ML bootstrap consensus trees inferred from

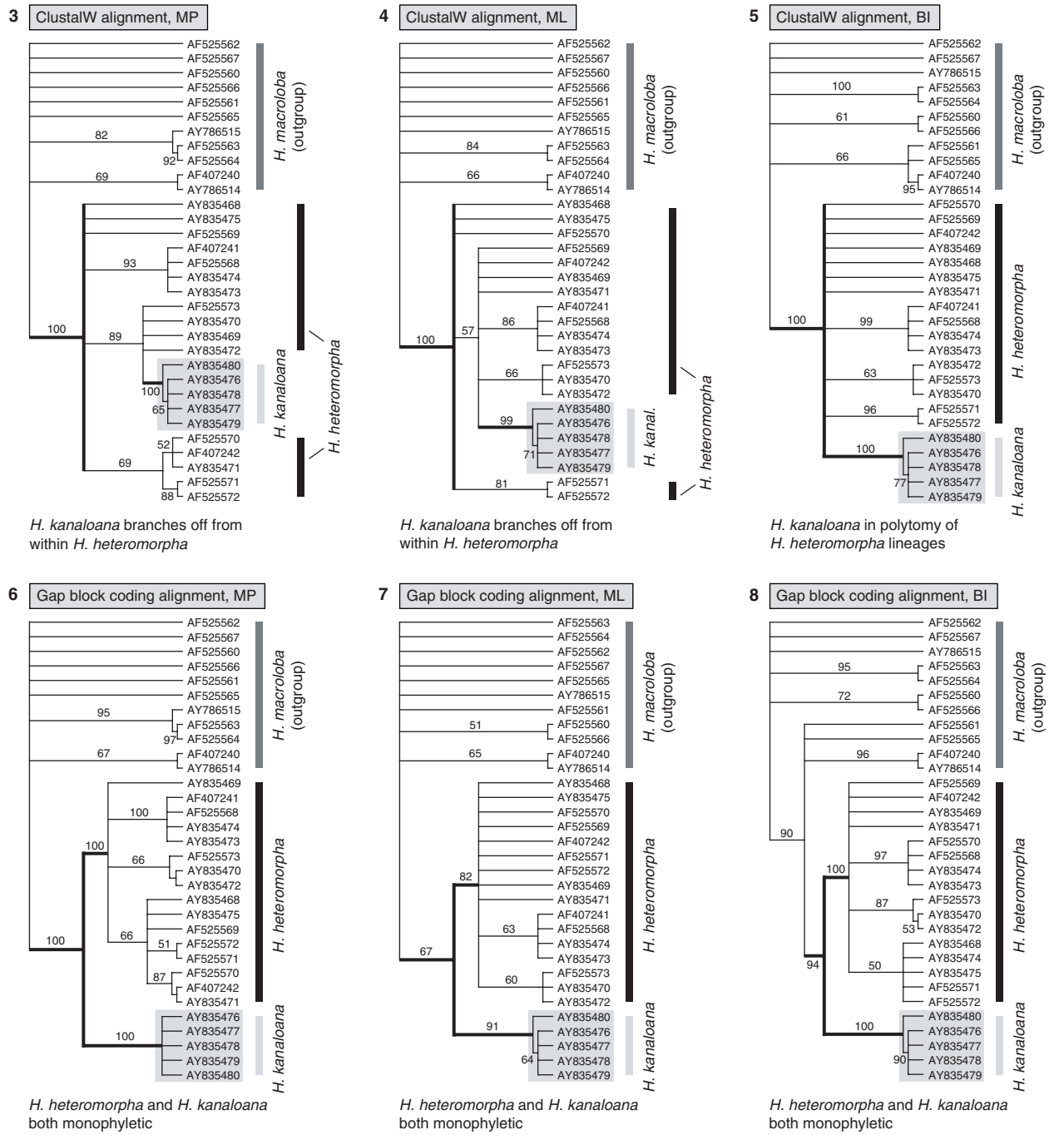

Figs 3–8. Fifty-percent majority rule consensus trees for MP, ML and Bayesian analyses of ITS1–ITS2 data aligned using different methods. Fig. 3. MP tree of ClustalW alignment. Fig. 4. ML tree of ClustalW alignment. Fig. 5. Bayesian tree of ClustalW alignment. Fig. 6. MP tree of gap block coding alignment. Fig. 7. ML tree of gap block coding alignment. Fig. 8. Bayesian tree of gap block coding alignment. Clade support is given as bootstrap proportions (ML and MP trees) and posterior probabilities (BI trees). Bold lines indicate the roots of *H. heteromorpha* and *H. kanaloana*.

the ClustalW alignment (Figs 3, 4), *H. kanaloana* branched off from within *H. heteromorpha*, leaving the latter paraphyletic. In the BI tree inferred from the ClustalW alignment (Fig. 5), the *H. kanaloana* clade formed a polytomy with all *H. heteromorpha* lineages, again suggesting that the latter species is paraphyletic. In all gap block coding alignment trees (Figs 6–8), *H. heteromorpha* and *H. kanaloana* formed well-supported, monophyletic lineages.

The alignment of *rps*3 sequences comprised 909 positions, individual sequences ranging from 672–828 bases long. The MrModeltest hLRT selected a general time-reversible model with substitution rates across sites following a gamma distribution (shape parameter 0.2721). Figures 9–11 show the 50% majority-rule consensus trees of the plastid *rps*3 data. *Halimeda kanaloana* and *H. heteromorpha* were both monophyletic, irrespective of the inference method.

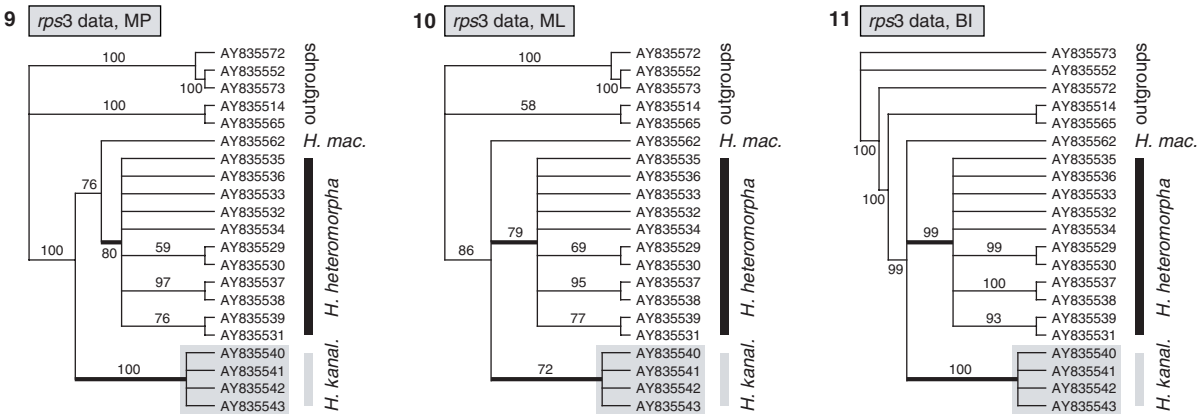

Figs 9–11. Fifty-percent majority rule consensus trees for MP, ML and Bayesian analyses of the *rps*3 alignment. Fig. 9. MP analysis. Fig. 10. ML analysis. Fig. 11. Bayesian analysis. Support is given as bootstrap proportions (ML and MP trees) and posterior probabilities (BI trees). Bold lines indicate the roots of *H. heteromorpha* and *H. kanaloana*.

Contrary to the ITS trees (Figs 3–8), *H. kanaloana* and *H. heteromorpha* did not cluster together in the *rps*3 trees. In the MP tree (Fig. 9), *H. heteromorpha* showed a sister relationship with *H. macroloba*. In the ML and BI trees (Figs 10, 11), the *H. heteromorpha*, *H. macroloba* and *H. kanaloana* clades arose from a single trifurcation.

The extended nrDNA data set suggests a sister relationship between *H. heteromorpha* and *H. kanaloana* (Fig. 1). A larger set of ITS1–ITS2 sequences throws the sister relationship into question (Figs 3–8; Verbruggen *et al.*, 2005*a*). Alternative alignments favour paraphyly (ClustalW: Figs 3–5) or monophyly (gap block coding: Figs 6–8) of *H. heteromorpha*. These topological discrepancies highlight the sensitivity of phylogenetic inference methods to alignment differences. Such difficulties are often encountered with ITS, due to the presence of indels, especially in areas lacking secondary structure conservation (Alvarez & Wendel, 2003). Verbruggen *et al.* (2005*a*) delineated species in *Halimeda* section *Rhipsalis* from DNA sequence data aligned automatically rather than manually to minimize subjectivity. The gap block coding alignment used in the present study is more conservative than the ClustalW alignment used by Verbruggen *et al.* (2005*a*) because sites or regions where interspecific sequence alignment was ambiguous were separated into sequence blocks, precluding non-homology of characters (bases) at the same alignment position. Our results suggest that the ClustalW algorithm with standard settings may not have provided the most appropriate alignment for inferring interspecific phylogenetic relationships because the more conservative gap block coding alignment of the ITS1–ITS2 data and the *rps*3 data both suggest that *H. heteromorpha* and *H. kanaloana* are monophyletic.

In the Pacific Ocean, *H. heteromorpha* occurs only in southern hemisphere archipelagos whereas *H. kanaloana* is limited to the northern hemisphere (Hawai'i and probably the Ryukyu islands, Fig. 71). The most credible topologies for the *H. heteromorpha–kanaloana–macroloba* species group (based on the longest sequence alignments, Figs 1, 2) show *H. macroloba* branching off first, leaving *H. heteromorpha* and *H. kanaloana* as closest relatives. There are several examples of sibling species that have non-overlapping ranges in the north and south Pacific (Palumbi, 1997; Bernardi *et al.*, 2001; Bay *et al.*, 2004). Such distributions could have originated by cross-equatorial jump dispersal (Rotondo *et al.*, 1981). Considering the inhibition of cross-equatorial dispersal by the equatorial counter current (Tomczak & Godfrey, 2003), limited gene flow is expected between putative founder populations in northern and southern Pacific populations, leading to morpho-ecological and DNA sequence divergence.

Species boundaries: comparative morphology

Perception and accurate delineation of species is one of the major issues facing algal systematists. Molecular phylogenetic techniques have provided a new perspective on algal diversity and have revealed poorly defined species boundaries in all marine algal groups (e.g. van der Strate *et al.*, 2002; Gurgel *et al.*, 2003; Zuccarello & West, 2003; Cohen *et al.*, 2004; Yano *et al.*, 2004; De Clerck *et al.*, 2005; Kooistra & Verbruggen, 2005). Establishing diagnostic differences requires sequencing numerous specimens and examining disregarded morphological variability. In *Halimeda* section *Rhipsalis*, DNA sequencing and morphometric methods have been combined to pinpoint species differences (Verbruggen *et al.*, 2005*a*). Based on

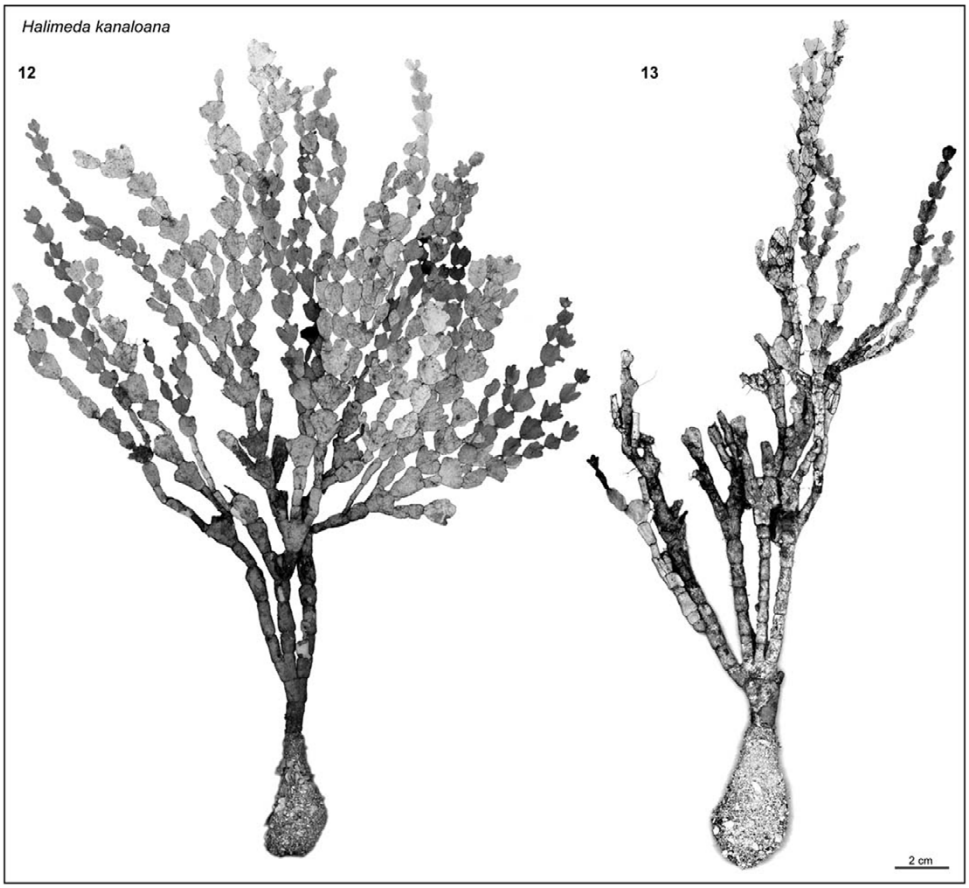

Figs 12–13. *Halimeda kanaloana* thalli. Fig. 12. BISH715565 (holotype) from Mau'i, Hawai'i. Fig. 13. HS-2004-161 from Mau'i, Hawai'i.

these results, we now describe the morphological differences between the focal species of this study and provide detailed descriptions at the end of the paper. It must be stressed that cited dimensions refer to median values of ten replicate measurements, as described in Verbruggen *et al.* (2005*a*, *c*). This approach narrows the range of values obtained because median values are not heavily impacted by outliers. As a consequence of the narrower ranges, species overlap is small or disappears entirely, and boundaries between species can be more easily defined even when specimens at the edges of the morphological range are included. The advantage of using the median range instead of the actual range of measurements makes identification more straightforward and less ambiguous. We encourage the use of medians from a series of replicate measurements as a standard in *Halimeda* taxonomy and identification.

The four focal species are illustrated in Figs 12–70 and their main features and morphometric measurements summarized in Table 1. The most obvious difference between the four species is the presence or absence of a bulbous holdfast. Whereas *H. kanaloana* and *H. incrassata* are anchored in sand by means of a massive bulb composed of rhizoids and sand (Figs 12–13, 27–31), *H. melanesica* and *H. heteromorpha* are attached to rocky substrata by a felt-like mat of rhizoids (Figs 14–16, 19–21, 32–35). However, relying on this character to distinguish between these species pairs is not without danger. Collections may lack holdfasts, rendering the character useless, or holdfasts may vary in shape and structure depending on environmental conditions (Verbruggen & Kooistra, 2004). For instance, *H. heteromorpha* can exhibit a more elaborate holdfast when growing on silt- or sand- covered rock (Figs 14, 15), *H. melanesica* is known occasionally to form bulbous holdfasts (e.g. HEC5671, GENT), and *H. kanaloana* has a reduced holdfast when growing on sand-covered rock (pers. obs.).

Halimeda incrassata and *H. kanaloana* both have many large pores at nodes. There are several diagnostic features separating these two species: (i) subperipheral utricles of *H. kanaloana* are markedly inflated while those of *H. incrassata* are not (Fig. 49 *v.* 55); (ii) the median distance between the base of the nodal fusions and the first siphon ramification above the node (supranodal siphon) is larger in *H. kanaloana* than in *H. incrassata* (Fig. 39 *v.* 44); (iii) peripheral utricles of *H. incrassata* tend to be smaller than those of *H. kanaloana* (Figs 49, 50 *v.*

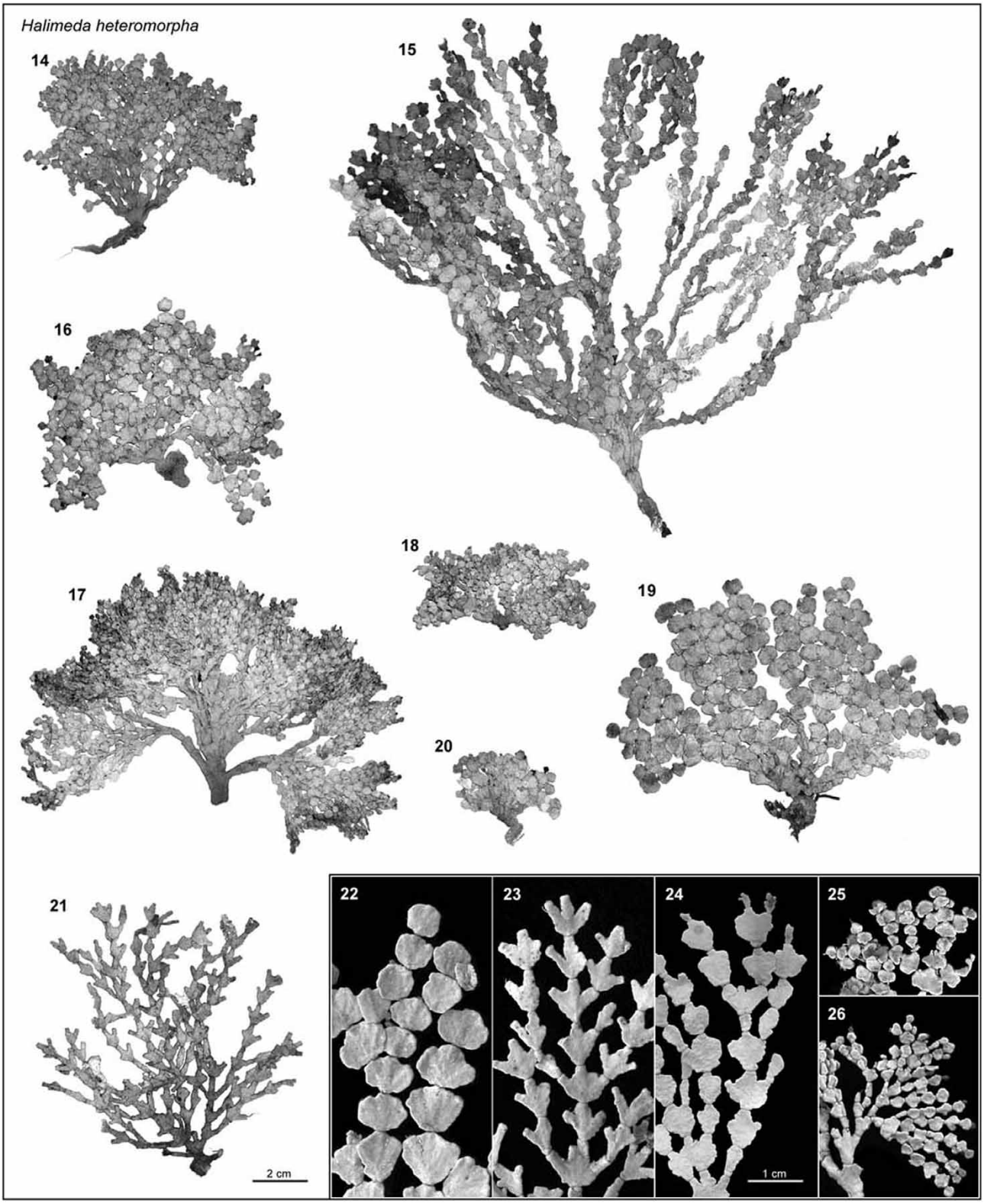

Figs 14–26. *Halimeda heteromorpha* thalli from different localities. Fig. 14. HV231, French Polynesia. Fig. 15. HV22, Zanzibar. Fig. 16. HV144, French Polynesia. Fig. 17. HV146, French Polynesia. Fig. 18. HV104, French Polynesia. Fig. 19. HV629, The Philippines. Fig. 20. HV636, The Philippines. Fig. 21. HV763, The Philippines. Fig. 22. HV629, The Philippines. Fig. 23. SHV763, The Philippines. Fig. 24. HV22, Zanzibar. Fig. 25. HV104, French Polynesia. Fig. 26. HV146, French Polynesia. 2-cm scale bar applies to Figs 14–21; 1-cm bar to all insets, Figs 22–26. All specimens from the Ghent University Herbarium (GENT).

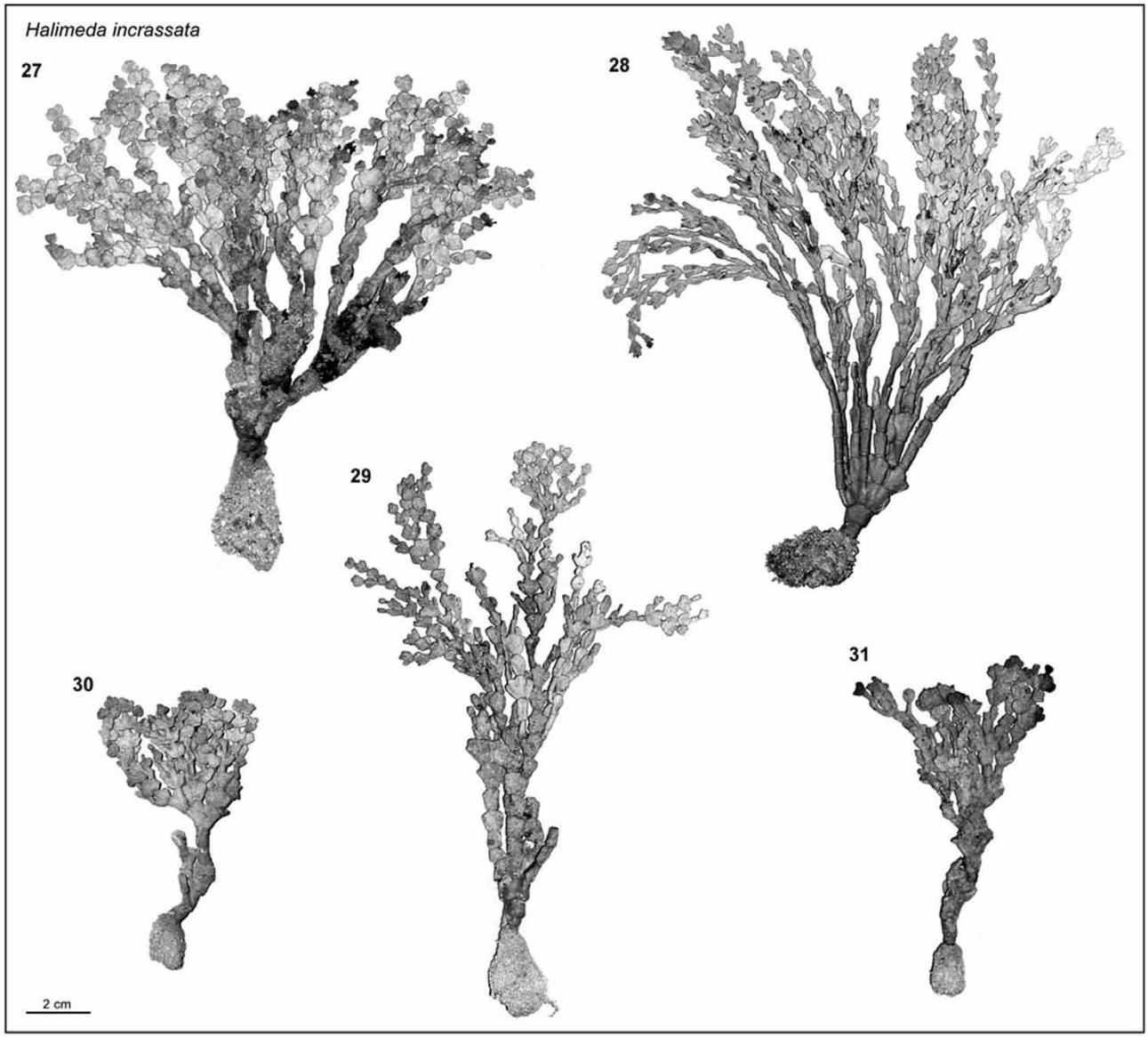

Figs 27–31. *Halimeda incrassata* thalli from different locations. Fig. 27. HOD-MAR01-42, Martinique. Fig. 28. S H.0667, Panama. Fig. 29. HV978, Jamaica. Fig. 30. H.0666, Panama. Fig. 31. HV899, Jamaica. All specimens from the Ghent University Herbarium (GENT).

55, 56); (iv) observed in surface view, *H. incrassata* has slightly rounded peripheral utricles whereas *H. kanaloana* utricles consistently have angular corners (Fig. 56 *v.* 50; (v) from an ecological point of view, *H. incrassata* favours shallow sites (seagrass beds, mangroves, shallower parts of reef slopes) whereas *H. kanaloana* is known from deeper sand and rubble flats (15 to > 85 m deep) where it often forms quasi-monospecific stands; (vi) the distribution ranges of *H. incrassata* and *H. kanaloana* do not overlap: the former is restricted to the Atlantic and the latter known only from the North Pacific Ocean (Fig. 71).

Halimeda incrassata and *H. heteromorpha* differ in a number of obvious characters: (i) *H. incrassata* is anchored in sand by means of a large, sand-encrusted bulbous holdfast (Figs 27–31) whereas *H. heteromorpha* is attached to rock or silt-covered rock by a much smaller, felt-like holdfast (Figs 14–16, 19–21); (ii) *H. incrassata* features a relatively high nodal adhesion belt with many obvious, large pores while *H. heteromorpha* has a narrower adhesion belt with diminutive pores (Fig. 45 *v.* 42, 43; (iii) less conclusive differences include the length of the supranodal siphon (Fig. 41 *v.* 44) and the diameter of peripheral utricles (Fig. 58 *v.* 52, 54), which both tend to be smaller in *H. incrassata* than in *H. heteromorpha*; (iv) whereas *H. incrassata* grows on sand (mostly in seagrass beds and mangroves), *H. heteromorpha* grows on rocky substrata in a variety of habitats; (v) *H. incrassata* is a strictly Atlantic species whereas *H. heteromorpha* is restricted to the Indo-Pacific basin.

Halimeda heteromorpha and *H. kanaloana* are closely related species within a well-supported

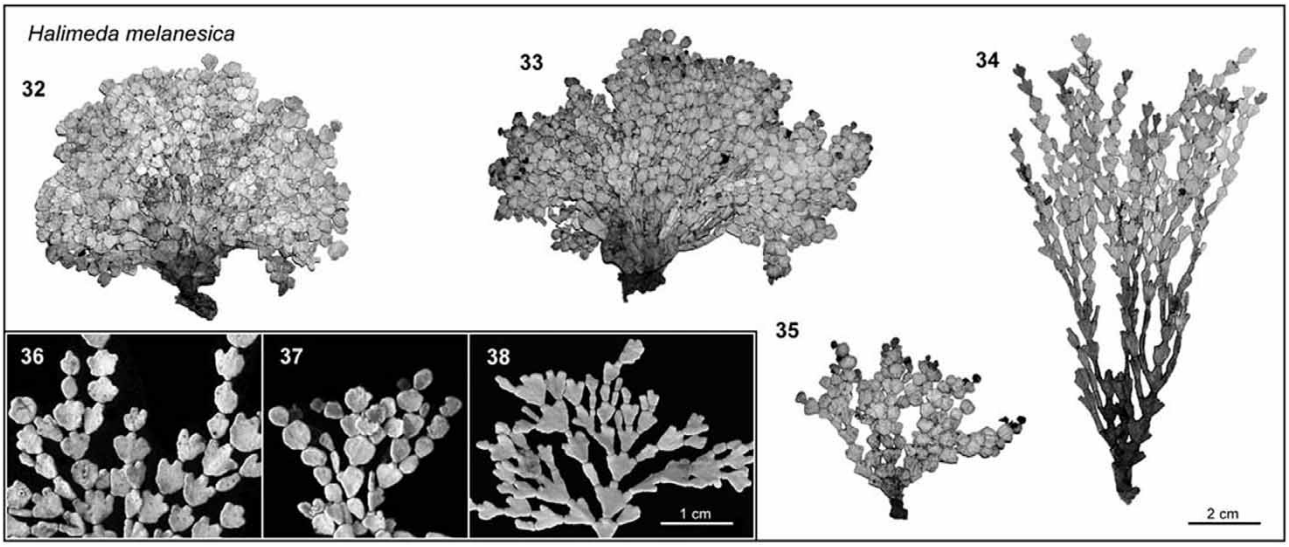

Figs 32–38. *Halimeda melanesica* thalli from different locations. Fig. 32. HV818, The Philippines. Fig. 33. HV217, French Polynesia. Fig. 34. HV790, The Philippines. Fig. 35. HV217, French Polynesia. Fig 36. HV790, The Philippines. Fig 37. HV217, French Polynesia. Fig. 38. L.0399626, Indonesia. All specimens from Ghent University Herbarium (GENT) except L.0399626, which is from NHN-Leiden (L).

clade that also contains *H. macroloba* (see above). *Halimeda heteromorpha* differs from the other species in having a felt-like, non-bulbous holdfast and reduced nodal fusions (Figs 14–16, 18–21 *v.* 12–13). Peripheral utricles of *H. heteromorpha* and *H. kanaloana* are almost identical in dimensions, but those of *H. kanaloana* tend to broaden nearer their base (Fig 49 *v.* 51, 53). More specifically, utricles of *H. kanaloana* are more than 42% of their maximal width a quarter length from their base, which is rarely the case in *H. heteromorpha*. Subperipheral utricles in *H. kanaloana* are markedly inflated unlike those of *H. heteromorpha* (Fig 49 *v.* 51, 53). In this respect, *H. kanaloana* resembles *H. macroloba* (Figs 59, 60). Reproductively, *H. macroloba* and *H. kanaloana* both produce gametophores from internal medullar siphons, although gametophores in *H. kanaloana* are longer and thicker than in *H. macroloba*. *H. heteromorpha*, *H. kanaloana* and *H. macroloba* also differ from an ecological and geographic perspective. Whereas *H. macroloba* is a sand-growing species restricted to shallow, lagoon habitats, *H. kanaloana* is a sand-dwelling species that occurs most commonly in deep water habitats. *Halimeda heteromorpha* grows on rock at relatively shallow sites. Our observations indicate that reproduction in *H. macroloba* and *H. kanaloana* occurs almost continuously, with small proportions of the populations fertile for many months of the year (see also Merten, 1971). Contrastingly, no fertile *H. heteromorpha* was found in our collections. *Halimeda heteromorpha* occurs throughout the tropics in the Indian Ocean and the South Pacific, but does not seem to overlap with *H. kanaloana*, known only from Hawai'i and the Ryukyu Islands (i.e. northern Pacific Ocean). *Halimeda macroloba* occurs throughout the Indo-Pacific (Hillis-Colinvaux, 1980), including the Ryukyu Islands (Tsuda & Kamura, 1991) and Hawai'i (Abbott & Huisman, 2004).

Halimeda heteromorpha and *H. melanesica* differ from the remainder of the section by their reduced nodal fusion pattern (Figs 41–43, 46–48) and epilithic habit with a matted holdfast. Their segment morphology can be extremely similar. The trilobed segments of *H. melanesica* specimens from surge-affected sites (Fig. 38) can be very similar to those of *H. heteromorpha* from fore-reef slopes (Fig. 23), and segments of the wave-affected form of *H. melanesica* (Fig. 37) show a striking resemblance to those of lagoon forms of *H. heteromorpha* (Figs 25, 26). Nonetheless, there are a few anatomical characters that allow identification: (i) peripheral utricles are smaller in *H. melanesica* (Figs 52, 54 *v.* 58); (ii) the subperipheral utricles are markedly more slender in *H. melanesica* – the median diameter of secondary utricles is 42–66 μm in *H. heteromorpha* but 32–45 μm in *H. melanesica*. The height of the secondary utricles does not differ significantly between the species, causing the secondary utricles of *H. melanesica* to appear more slender (Figs 51, 53 *v.* 57).

Some ecotypes of *H. heteromorpha* could be confused with more distantly related species. For example, specimens with round segments (Figs 19, 22) resemble *H. tuna* (Ellis & Solander) Lamouroux and *H. discoidea* from *Halimeda* section *Halimeda*, and *Halimeda bikinensis*

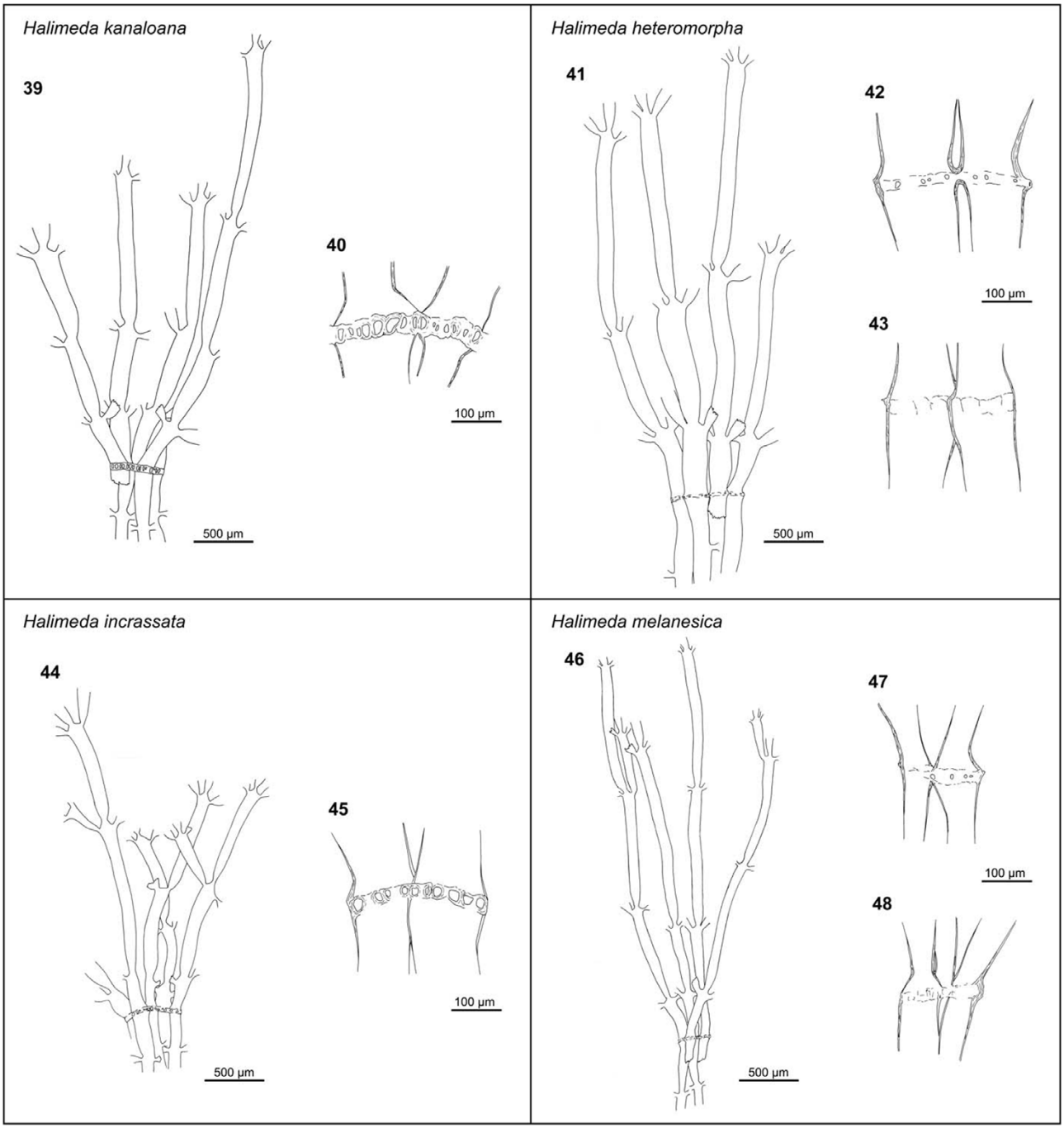

Figs 39–48. Medullar and nodal features. Figs 39–40. *H. kanaloana*, H.0649. Fig. 39. Medulla. Fig. 40. Detail of nodal siphon fusion. Figs 41–43. *H. heteromorpha*. Fig. 41. Medulla, HV629. Fig. 42. Detail of nodal siphon fusion, HV629. Fig. 43. Detail of nodal siphon adhesion, HV636. Figs 44–45. *H. incrassata*, HV448. Fig. 44. Medulla. Fig. 45. Detail of nodal siphon fusion. Figs 46–48. *H. melanesica*. Fig. 46. Medulla, HV818. Fig. 47. Detail of nodal siphon fusion, HV818. Fig. 48. Detail of nodal fusion, HV217. All specimens from the Ghent University Herbarium (GENT).

Taylor, whose relationship to the current sections is unclear (Verbruggen & Kooistra, 2004). However, anatomical characters allow unequivocal distinction between the discoid *H. heteromorpha* and the other species. The most evident character in this context is nodal fusion pattern. Whereas all medullar siphons in *H. heteromorpha* adhere into a single unit sometimes interconnected by small pores, nodal siphons show complete fusion in pairs or triplets throughout *Halimeda* section *Halimeda* and in *H. bikinensis* (Verbruggen & Kooistra, 2004). Trilobed *H. heteromorpha* (Figs 21, 23) can superficially resemble trilobed specimens of *Halimeda minima* (Taylor) Colinvaux, *Halimeda goreauii* Taylor or *Halimeda distorta* (Yamada) Hillis-Colinvaux from *Halimeda* section *Opuntia* (Kooistra & Verbruggen, 2005); however, fusion of nodal siphons into a single unit clearly differentiates *H. heteromorpha* from these species. Species in the section *Opuntia* show

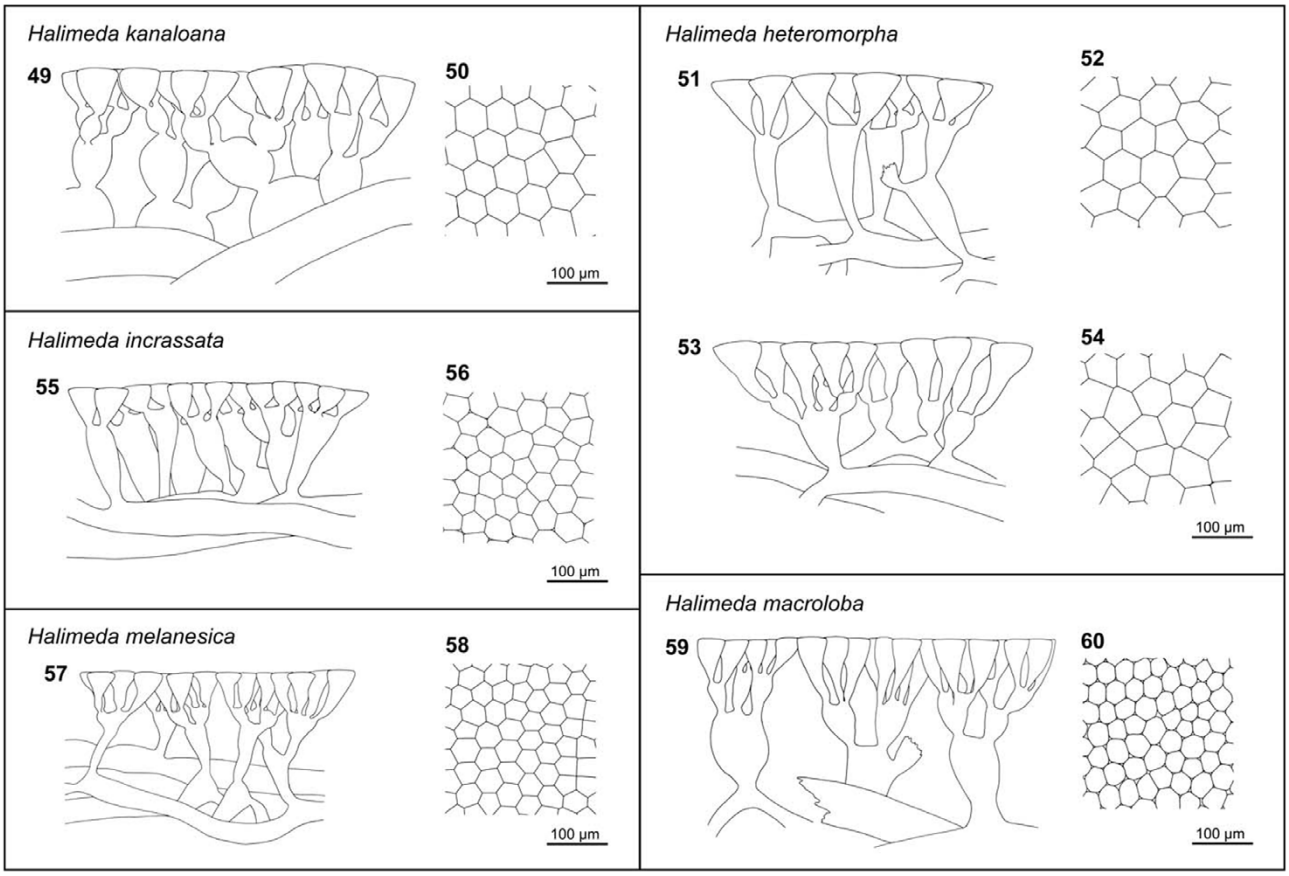

Figs 49–60. Cortical features in cross-section and surface views. Figs 49, 50. *H. kanaloana*, H.0649. Fig. 49. Cross-section. Fig. 50. Surface. Figs 51–54. *H. heteromorpha*. Fig. 51. HV22, cross-section. Fig. 52. HV22, surface. Fig. 53. HV763, cross-section. Fig. 54. HV763, surface. Figs 55, 56. *H. incrassata*, HV332. Fig. 55. Cross-section. Fig. 56. Surface. Figs 57, 58. *H. melanesica*, HV818. Fig. 57. Cross-section. Fig. 58. Surface. Figs 59, 60. *H. macroloba*, HV206. Fig. 59. Cross-section. Fig. 60. Surface. All specimens from the Ghent University Herbarium (GENT).

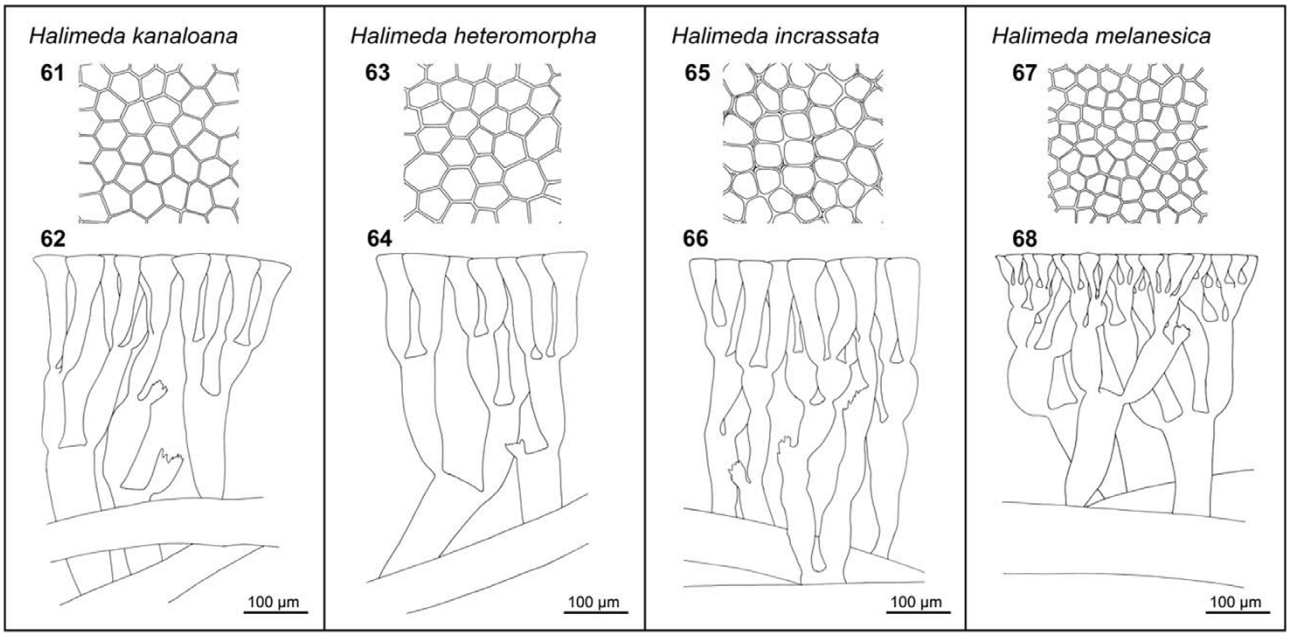

Figs 61–68. Cortical features of basal segments in cross-section and surface views. Figs 61, 62. *H. kanaloana*, H.0653. Fig. 61. Surface. Fig. 62. Cross-section. Figs 63, 64. *H. heteromorpha*, HV146. Fig. 63. Surface. Fig. 64. Cross-section. Figs 65, 66. *H. incrassata*, HV448. Fig. 65. Surface. Fig. 66. Cross-section. Figs 67, 68. *H. melanesica*. Fig. 67. Surface, HV818. Fig. 68. Cross-section, HV790. All specimens from the Ghent University Herbarium (GENT).

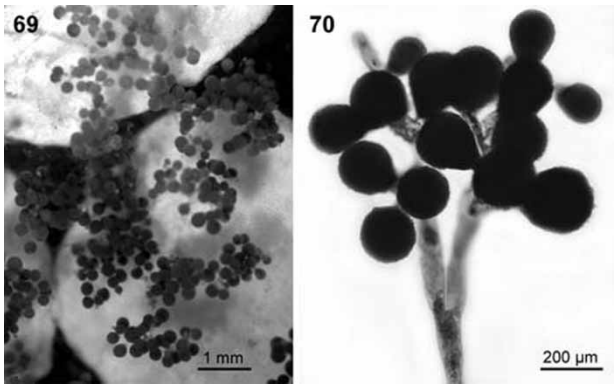

Figs 69–70. Fertile *H. kanaloana*, HS 2004-162 (personal herbarium of Heather Spalding, to be deposited in the Bishop Museum). Fig. 69. Position of gametangia along margins and on segment surfaces. Fig. 70. Detail of gametophore.

incomplete fusion in pairs, triplets or small groups (Verbruggen & Kooistra, 2004).

The use of the anatomy of basal, stipitate segments in species delineation remains enigmatic. Both Noble (1986) and Dragastan *et al.* (2002) considered these segments diagnostically useful. However, Verbruggen *et al.* (2005*d*) showed that inclusion of basal segments in morphometric data sets impaired the accuracy of automated identification. Despite this, it was argued that basal segment anatomy may be useful when coded as a separate set of variables. Treated thus, basal segment information would aid species identification without conflicting with diagnostic characters from more apical segments. Nodal fusion in the *H. incrassata* complex studied here did not usually differ between basal and more apical segments. However, the appearance and size of peripheral and subperipheral utricles did differ between basal and more apical segments; utricles of basal segments were more rigid, thick-walled and elongate than those mid-thallus. Whether this is determined by segment function (thallus support), age (basal segments are older) or both is unclear. Although none of the focal species of this study could be recognized on the basis of basal segment anatomy alone, differences in size and rounding of peripheral utricles in normal segments were seen in basal segments, too. We did not attempt morphometric analysis of basal segments.

Nomenclature and taxonomy

Halimeda tridens (Ellis & Solander) Lamouroux and *Halimeda brevicaulis* Kützing, both synonyms of *H. incrassata*, were originally described from Atlantic collections and, although the name *H. tridens* was subsequently applied to Indo-Pacific material (e.g. Taylor, 1950), our molecular analysis shows that neither name is appropriate for Pacific specimens. *Halimeda polydactylis* J. Agardh, a species of Pacific origin, was treated as a synonym of *H. incrassata* by Barton (1901) but later transferred to *H. cylindracea* (Hillis, 1959). *Halimeda triloba* Decaisne was illustrated by Kützing (1857) with a mixture of specimens similar to *H. opuntia* and *H. incrassata*. However, according to Barton (1901), Decaisne's type material belongs to *H. opuntia*. As a consequence *H. triloba* is not relevant to the nomenclature of *H. incrassata*-like species.

Halimeda heteromorpha is an amalgam of different forms, several of which had been described as forms or varieties of *H. incrassata*. *Halimeda incrassata* var. *ovata* J. Agardh (= *H. incrassata* f. *ovata*) conforms to specimens from lagoonal habitats (Figs 14, 16–18), *H. incrassata* f. *tripartita* Barton probably conforms to specimens from sheltered fore-reef slopes (Figs 21, 23) and *H. incrassata* f. *rotunda* Barton to specimens from surge-affected sites (Figs 19, 22). Even though we have not studied the specimens Barton (1901) used for her descriptions, her illustrations are fairly conclusive. Rather than raising one of her forms to specific rank, we have chosen a new epithet *heteromorpha*, because the earlier intraspecific names imply shape characteristics that are not diagnostic for this species as a whole. Furthermore, the various forms have been a source of confusion. For example, *H. incrassata* f. *ovata* was applied to specimens belonging to *H. borneensis* (Payri & Meinesz, 1985; Payri *et al.*, 2000). We decided not to maintain or erect any infraspecific taxa because molecular support is lacking and several intermediate morphologies exist in the collections studied (cf. Figs 22–24).

Specimens of *H. heteromorpha* have often been mistaken for *H. melanesica* based on similar holdfast type and nodal fusion pattern (e.g. Noble, 1987; Dargent, 1997; Verbruggen & Kooistra, 2004). Literature reports of *H. melanesica* should therefore be scrutinized. In the original description of *H. melanesica* (Valet, 1966), no comparison was made with specimens of the *H. incrassata* group.

Cryptic and pseudo-cryptic diversity

Cryptic species, sometimes referred to as sibling species, are defined as species that are impossible to distinguish based on morphological characters (Knowlton, 1993; Sáez & Lozano, 2005). Pseudo-cryptic species are species that are readily distinguished morphologically, once appropriate characters are considered. Although different clues may reveal (pseudo-) cryptic diversity, DNA sequence analysis is currently most commonly

used, as for *H. incrassata* and many other marine algae (e.g. van der Strate *et al*., 2002; Cohen *et al*., 2004; De Clerck *et al*., 2005).

Whether a discovery of hidden diversity should be described as cryptic or pseudo-cryptic is subjective, depending on the effort required to find morphological differences (Sáez *et al*., 2003). This is well exemplified by *H. incrassata*. Kooistra *et al*. (2002) found two discrete entities on the basis of nuclear ribosomal DNA data, and a third was recognized by Verbruggen *et al*. (2005*a*) on the basis of nuclear ITS and plastid *rps*3. Although initially regarded as cryptic species, morphometric analyses revealed several morphological differences (Verbruggen *et al*., 2005*a*; this study).

Additional pseudo-cryptic entities may be discovered within the *H. incrassata* complex. For example, Indo-Pacific specimens illustrated by Tseng (1984) and South (1992) do not appear to belong to *H. kanaloana* or *H. heteromorpha*. The same is true for an entity from Papua New Guinea in the Ghent University Herbarium (Coppejans *et al*., 2001) and one from Micronesia in the US National Herbarium (Smithsonian Institution). Because we did not have access to appropriately preserved specimens for DNA analysis, we cannot determine whether the entities in question represent further pseudo-cryptic entities or additional morphological variation within *H. heteromorpha*, *H. kanaloana* or *H. melanesica*.

Species descriptions

Halimeda kanaloana *Vroom, sp. nov. (Figs 12, 13, 39, 40, 49, 50, 61, 62, 69–70)*

Diagnosis: *Halimeda kanaloana Vroom a speciebus affinibus differt haptero magno bulboso in arenis specimen adfigente, parte thalli basali e segmentis magnis cylindricis vel paulo complanatis constante, segmentis magnis trilobis obovoideis vel cuneatis in partibus thalli centralibus distalibusque (longitudine mediana 9–14 mm, latitudine 6–11 mm, crassitie 1.5–2.9 mm), siphonibus medullaribus ad segmentorum nodos in unum conjungentibus, poris manifestis ad segmentorum nodos connectentibus siphones adjacentes (altitudine pororum mediana 47–69 μm parietibus cellularum inclusis), stratis utriculorum 4–5, utriculis peripheralibus magnis (diametro mediano 56–73 μm, altitudine 69–98 μm) attingentibus 42% suae maximae latitudinis ad quartem partem altitudinis suae et a superficie visis angulis rotundatis semper carentibus, et utriculis subperipheralibus valde inflatis*.

Halimeda kanaloana Vroom differs from related species through the combination of a large bulbous holdfast anchoring the specimen in sand, a basal thallus region of massive cylindrical to slightly flattened segments, large obovoid to cuneate trilobed segments in the central and distal thallus regions (median length 9–14 mm, width 6–11 mm, thickness 1.5–2.9 mm), medullar siphons fusing into a single unit at segment nodes, obvious pores connecting neighbouring siphons at segment nodes (median pore height including cell walls 47–69 μm), 4–5 utricle layers, large peripheral utricles (median diameter 56–73 μm, height 69–98 μm) that reach 42% of their maximal width at a quarter of their height and do not have rounded corners in surface view, and markedly inflated subperipheral utricles.

Holotype: BISH715565 (BISH). Collected at Keyhole, Mau'i, Hawai'i, USA. Growing in a monospecific meadow at a depth of 56 m. Collected on 6 September 2004, during dive 565 of the submersible Pisces V.

Paratypes: H.0649 through H.0658 (GENT), Honolua Bay, Mau'i, Hawai'i, USA. HS-2004-162, HS-2004-171, HS-2004-173 through HS-2004-178 from Keyhole, Mau'i, Hawai'i, USA. HS-2004-157, HS-2004-159, HS-2004-161 from Kaho'olawe, Hawai'i, USA.

Etymology: The epithet *kanaloana* means belonging to Kanaloa, the Hawai'ian god of the ocean.

Description: *Halimeda kanaloana* forms extensive meadows in sandy environments. Occasional individuals are found as shallow as 1–2 m, with dense stands beginning at 15 m and ending abruptly around 85 m. Specimens are anchored in sand by means of a gritty, bulbous anchoring holdfast, up to 8 cm in length (Figs 12, 13), within which the rhizoids cling tightly to sand. Very rarely, specimens are found attached to rock.

The heavily calcified stipe is sparsely branched and, in older specimens, overgrown by sponges, encrusting coralline algae, and filamentous algal epiphytes (Figs 12, 13). The basal thallus region consists mainly of squat cylindrical segments with some bilobed and laterally fused segments that produce additional branches (Figs 12, 13). Most branching occurs mid-frond, just above the basal region (Figs 12, 13). In the central region, axes often contain long series of less heavily calcified, trilobed segments, several of which produce branches (Figs 12, 13). Young segments located towards the branch apices are lightly calcified and often become crumbly in herbarium presses.

Centrally located segments have median lengths of 9–14 mm and median widths of 6–11 mm, with median length to width ratios of 1.02–1.48, and median thickness of 1.5–2.9 mm. Most segments from the central and apical thallus parts are obovate–cuneate (88%), broadest at or near their tip rather than at or near their base. The segment base is always acute. About one-third of the

segments are obovate and unlobed. The remaining segments are shallowly to deeply lobed. Of the lobed segments, the majority are trilobed (56%) or bilobed (29%). Lobed segments usually produce a branch from each lobe; trilobed segments with only two branches usually have a reduced third lobe.

Medullar siphons adhere into a single unit at segment nodes and individual siphons cannot be isolated from this unit without sectioning it. Dissected nodes feature a marked belt of thickened cell wall material (Figs 39, 40) of 47–69 μm median height, which is perforated by numerous large pores (Fig. 40). Median distance from the base of nodes to the first medullar ramification of the segment (supranodal siphon length) is 391–614 μm; its median diameter is 148–170 μm. Medullar siphons trifurcate; they rarely branch dichotomously (Fig. 39). Median medullar siphon diameters are 123–161 μm, with median length to width ratios of 7.8–10.6.

The cortex comprises 4–5 utricle layers (Fig. 49). Peripheral utricles adhere to one another at their distal ends, remaining firmly attached after decalcification. In surface view, peripheral utricles are arranged in a non-uniform pattern of polygons (Fig. 50) and never have rounded corners. Median peripheral utricle diameters and heights are 56–73 μm and 69–98 μm, respectively, with median height to diameter ratios of 1.08–1.51. Subperipheral utricles exhibit markedly inflated morphologies (Fig. 49). Median secondary utricle diameters and heights are 51–58 μm and 67–99 μm, respectively, with median height to diameter ratios of 1.29–1.78.

Compared with segments in more apical regions of the thallus, stipe segments have rigid, thick-walled, elongate utricles (Fig. 62). The thicker cell walls are obvious in surface view (Fig. 61). Siphon fusion at nodes in the lower thallus regions is similar to that in more apically situated nodes.

Halimeda kanaloana is holocarpic with reproductive individuals found in low numbers during many months of the year. Transparent gametophores are 2.7–3.4 mm long, 50–90 μm wide, and are produced from medullar siphons that are pushed through tiers of utricles before emerging from the cortex. Although reproductive structures form on all surfaces of bleached segments, they are often concentrated on terminal edges (Fig. 69). Gametophores usually exhibit 1 or 2 dichotomies about halfway along their length, separating the terminal, deeply pigmented gametangia into 2–3 distinct clusters (Fig. 70). Eight to 25 gametangia commonly occur on each gametophore with diameters ranging from 100–320 μm. The gametophore branches dichotomously several more times in each gametangial cluster. Each cluster contains a conspicuous discharge papilla.

DISTRIBUTION: *Halimeda kanaloana* forms extensive meadows between the islands of Mau'i, Kaho'olawe, Lana'i and Moloka'i in the main Hawai'ian islands (Abbott & Huisman, 2004, as *H. incrassata*). Specimens attributed to *H. incrassata* from the Ryukyu Islands, Japan (Tsuda & Kamura, 1991) probably also represent *H. kanaloana*. A distribution map is presented in Fig. 71.

Halimeda heteromorpha *N'Yeurt, sp. nov.* *(Figs 14–26, 41–43, 51–54, 63, 64)*

DIAGNOSIS: *Halimeda heteromorpha N'Yeurt a speciebus affinibus differt haptero implexo in saxis specimen adfigente, siphonibus medullaribus ad segmentorum nodos in unum conjungentibus, poris ad segmentorum nodos connectentibus segmenta adjacentia omnino nullis vel parvis (altitudine pororum mediana 25–36 μm parietibus cellularum inclusis), stratis utriculorum 2–3, utriculis peripheralibus magnis (diametro mediano 57–79 μm, altitudine 74–102 μm) non vulgo attingentibus 42% suae maximae latitudinis ad quartem partem altitudinis suae et a superficie visis angulis rotundatis semper carentibus, et utriculis subperipheralibus non manifeste inflatis.*

Halimeda heteromorpha N'Yeurt differs from related species through the combination of a matted holdfast attaching the specimen to rock, medullar siphons adhering into a single unit at segment nodes, total absence of pores connecting neighbouring segments at segment nodes or smallish nodal pores (median pore height including cell walls 25–36 μm), 2–3 utricle layers, large peripheral utricles (median diameter 57–79 μm, height 74–102 μm) that do not generally reach 42% of their maximal width at one fourth of their height and that never have rounded corners in surface view and subperipheral utricles that are not markedly inflated.

HOLOTYPE: HV149 (GENT). Collected between Papetoai and motu Tiahura, Moorea, French Polynesia. Growing at the base of a coral boulder on the landward side of the barrier reef, close to the reef crest.

PARATYPES: HV22, HEC12238 (GENT), Chwaka Bay, Zanzibar, Tanzania. HEC11946, HEC12065 (GENT), Matemwe, Zanzibar, Tanzania. HV104, HV144, HV146 (GENT), Moorea, French Polynesia. UPF097 (UPF), Marquesas, French Polynesia. UPF097, 2808, 2809, 2815, 2823 (UPF), Tahiti, French Polynesia. UPF2803, 2810, 2814 (UPF), Moorea, French Polynesia. HV629, HV636, PH245 (GENT), Olango, Philippines. HV763 (GENT), Tangat, Philippines. L.0399613 (L), Panjang Island, Berau Archipelago, Indonesia.

ETYMOLOGY: The epithet *heteromorpha* refers to the variable external morphology of the species.

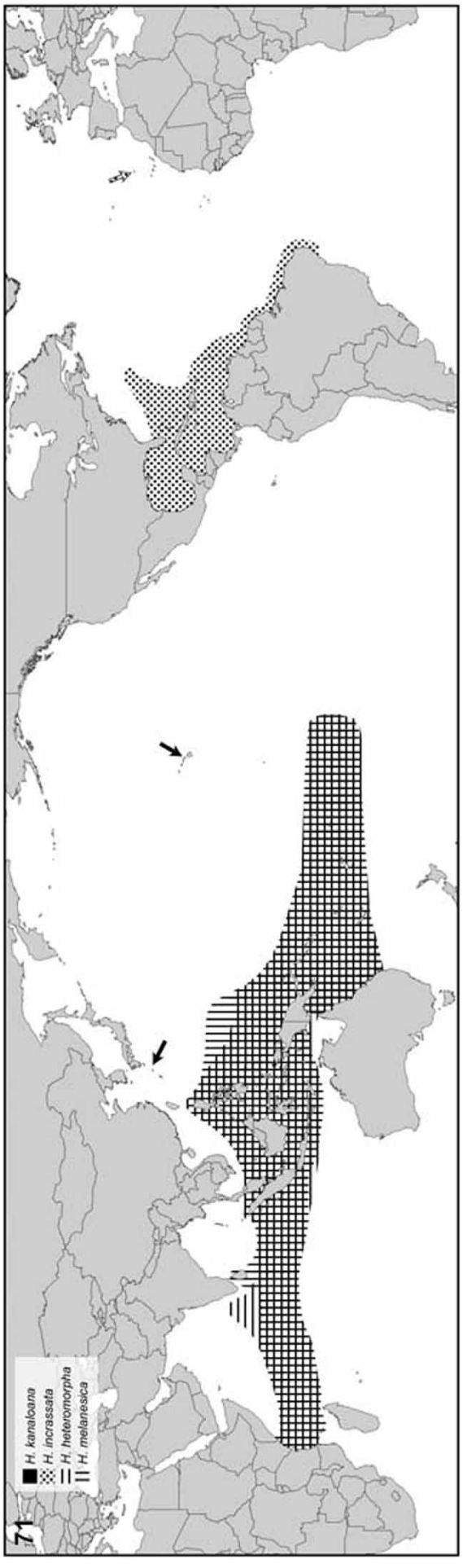

DESCRIPTION: *Halimeda heteromorpha* is characterized by highly variable ecology and morphology. It occurs in a broad spectrum of relatively shallow water habitats. Specimens are attached to rocky substrata by means of a rhizoidal mat of variable shape and consistency. In specimens that are directly attached to rock, the holdfast consists of a firm, dense mat of rhizoids (Figs 16, 19, 21). In specimens that grow on sand- or silt-covered rock, the holdfast zone is more flaccid (Figs 14, 15).

Specimens attached to rocky substrata in lagoonal habitats have several branches arising from the lowermost few segments (Figs 14, 16, 18). Segments are broader than long or about as broad as long (Fig. 25). Segment size diminishes from the base to the apices. Specimens that grow from within crevices in rock or coral boulders have a long, stipitate base composed of elongate, relatively thick segments (Fig. 17). Segments from the upper thallus are small, broader than long, or about as broad as long (Fig. 26). Specimens from extremely sheltered bays and mangrove channels are large and densely ramified close to their base (Fig. 15), although the resulting axes are sparsely branched. Specimens collected from shallow, surge-affected reef habitats consist of relatively large, round segments with more or less homogeneous branching throughout the thallus (Fig. 19). Specimens collected from sheltered fore-reef slopes have relatively large, trilobed segments with homogeneous branching throughout the thallus (Fig. 21). Finally, specimens collected from small crevices in rock boulders on reef flats that are exposed to vigorous tidal currents and moderate wave action exhibit diminutive thalli with relatively small segments (Fig. 20). Segments rarely merge in the basal zone (but see examples in Figs 17, 19).

Median lengths and widths of centrally located segments are 2.3–8.2 mm and 2.4–9.1 mm, respectively, with median length to width ratios of 0.66–1.16 and median thickness of 0.6–1.4 mm. Segments from specimens located in exposed habitats (Figs 19, 22), extremely sheltered bays

Fig. 71. Map showing the distributions of *H. heteromorpha*, *H. incrassata*, *H. kanaloana* and *H. melanesica*. Arrows indicate species findings outside the continuous distribution ranges. Note that *H. incrassata* s.l. and *H. melanesica* have been reported for several other Indo-Pacific localities. Given the taxonomic confusion, we only included localities from which we studied material, or where literature identifications were supported by illustrations and/or utricle measurements. Distribution ranges are uncertain for SE Asia, Madagascar and India-Sri Lanka, although large collections from Indonesia, the Philippines and Papua New Guinea were examined (GENT, L and US herbaria).

Table 1. Comparative table of features and morphometric measurements[a,b] of *Halimeda kanaloana*, *H. heteromorpha*, *H. incrassata* and *H. melanesica*

Character	*H. kanaloana*	*H. heteromorpha*	*H. incrassata*	*H. melanesica*
Holdfast	Bulbous, anchoring in sand	Felt-like mat, attaching to rock[c]	Bulbous, anchoring in sand	Felt-like mat, attaching to rock[c]
Median segment length	9–14 mm	2.3–8.2 mm	3.4–9.7 mm	3.8–5.5 mm
Median segment width	6–11 mm	2.4–9.1 mm	2.8–9.6 mm	4.0–5.4 mm
Median segment thickness	1.5–2.9 mm	0.6–1.4 mm	0.9–2.0 mm	0.7–0.9 mm
Anatomy of the nodal region	**Pores plentiful, large**	**Pores rare, diminutive**	**Pores plentiful, large**	**Pores rare, diminutive**
Median height of nodal adhesion band	**47–69 µm**	**25–36 µm**	33–53 µm	25–30 µm
Median length of supranodal siphon	**391–614 µm**	242–535 µm	**163–327 µm**	356–525 µm
Median diameter of supranodal siphon	148–170 µm	100–166 µm	95–150 µm	97–140 µm
Median medullar siphon diameter	123–161 µm	89–129 µm	85–153 µm	79–108 µm
Number of cortex layers	4–5	2–3	2–3	3
Peripheral utricles in surface view	Irregular polygons, all **corners angular**	Irregular polygons, all **corners angular**	Irregular polygons, **slightly rounded corners**	Irregular polygons, all **corners angular**
Median diameter of peripheral utricles	56–73 µm	**57–79 µm**	43–63 µm	**40–50 µm**
Median height of peripheral utricles	69–98 µm	74–102 µm	55–90 µm	40–53 µm
Appearance of subperipheral utricles	**Markedly inflated**	**Intermediate**	**Intermediate**	**Slender**
Median diameter of subperipheral utricles	51–58 µm	42–66 µm	42–67 µm	32–45 µm
Median height of subperipheral utricles	67–99 µm	54–111 µm	52–128 µm	49–92 µm
Habitat	Relatively deep sand and rubble flats	Variety of shallow-water, rocky habitats[c]	Shallow, sandy habitats	Surge-affected, rocky habitats
Distribution	North Pacific Ocean	Indian Ocean and South Pacific Ocean	**Atlantic Ocean**	Indian Ocean and South Pacific Ocean

[a] Dimensions represent the upper and lower median values of 10 replicate measurements per specimen (Verbruggen *et al.*, 2005*a*, *c*), from non-apical, calcified segments in the central and upper parts of the thallus (Verbruggen *et al.*, 2005*d*).
[b] Diagnostic characters are in boldface. Note that these characters are diagnostic only between the four studied species.
[c] Character shows some intraspecific variation. See text for details.

(Figs 15, 24) and sheltered fore-reef slopes (Figs 21, 23) lie at the high end of these ranges. The segment surfaces in the central and upper thallus are rough, often ruffled, especially in the small, upper segments (Figs 17, 18, 25, 26). Segments are moderately to poorly calcified and somewhat pliable, although specimens from surge-affected sites (Fig. 19) and the fore-reef slope (Fig. 21) have more strongly calcified segments with relatively pliable nodes. Segment shape is extremely variable among, and to a lesser extent within, ecotypes. In specimens from surge-affected sites, segments are more or less discoid (Figs 19, 22). In populations from fore-reef slopes, segments are markedly trilobed (Fig. 23). Finally, in specimens from lagoon habitats, the majority of segments are ovate–obovate (70%), with 32% of segments unlobed and 58% shallowly trilobed.

Medullar siphons adhere closely at nodes, an adhesion band visible in dissected nodes (Figs 41–43). Pores between parallel siphons are small (Fig. 42) or absent (Fig. 43). Median adhesion belt heights are 25–36 μm. Median supranodal siphon lengths and diameters are 242–535 μm and 100–166 μm, respectively. Medullar siphons trifurcate; they rarely branch dichotomously (Fig. 41). Median medullar siphon diameters are 89–129 μm, with median length to width ratios of 7.05–11.7.

The cortex consists of 2–3 utricle layers (Figs 51, 53). Peripheral utricles adhere to one another at their distal ends, remaining attached after decalcification. Median peripheral utricle diameters and heights are 57–79 μm and 74–102 μm, respectively, with median height to diameter ratios of 0.98–1.66. In surface view, peripheral utricles create a non-uniform pattern of polygons, without rounded corners (Figs 52, 54). Subperipheral utricles are not markedly inflated (Figs 51, 53). Median secondary utricle diameters and heights are 42–66 μm and 54–111 μm, respectively, with median height to diameter ratios of 1.09–2.05.

Cortex of thick, basal segments (see stipitate segments of specimen in Fig. 17) comprises more utricle layers than the upper segments (Fig. 64). Compared with central and apical thallus segments (cf. Figs 51, 53), stipitate segment utricles are more rigid, thick-walled and elongate. The thicker cell walls are particularly visible in surface view (Fig. 63). Siphon fusion at nodes is very similar in all thallus regions.

Distribution: *Halimeda heteromorpha* occurs throughout the tropical parts of the Indo-Pacific ocean basin. A compilation of distribution data based on specimens from the GENT, L, and UPF herbaria and literature reports (e.g. Barton 1901 as *H. incrassata* f. *ovata*, Noble 1987 as *H. melanesica*) is shown in Fig. 71.

Halimeda incrassata *(J. Ellis) J.V. Lamouroux (Figs 27–31, 44, 45, 55, 56, 65, 66)*

Holotype: The type specimen of *H. incrassata* has been lost (Barton, 1901; Hillis-Colinvaux, 1980).

Lectotype: The illustrations of Ellis (1767), which were reproduced in Hillis-Colinvaux (1980: p. 20), are hereby designated as the lectotype.

Description: *Halimeda incrassata* thalli are anchored in sandy substrata by means of a 2–5-cm long, bulbous holdfast comprising a network of rhizoidal siphons adhering to sand particles. The species inhabits a range of sandy-bottom habitats, including lagoons, seagrass beds, mangroves, and sand patches on outer reef slopes.

Thalli generally feature a sparsely branched, basal zone of thick, rigid segments (Figs 27–31). Neighbouring basal segments occasionally fuse (Fig. 28) and are often covered with a thick layer of epiphytes, particularly encrusting corallines (Figs 27, 29, 30). Major branches typically arise in the lower half of the thallus with more apically situated segments featuring flattened morphologies. Specimens collected from sheltered, low-light environments near the edge of mangrove swamps (Fig. 28) differ from average specimens by having large, fan-like bases composed of fused segments, from which many long branches arise.

Median lengths and widths of centrally located segments are 3.4–9.7 mm and 2.8–9.6 mm, respectively, with median length to width ratios of 0.69–1.43, and median thickness of 0.9–2.0 mm. The majority of segments are obovate–cuneate (79%), being broadest at or near their tip rather than at or near their base. The base is usually acute (61% of segments). Segments are unlobed (42%) or shallowly lobed (36%) with the majority of lobed segments trilobed (72%). Although all specimens feature both trilobed and unlobed segments, one type of segment morphology is usually dominant in a specimen.

Medullar siphons adhere into a single bundle at nodes and individual siphons cannot be separated from the bundle. Dissected nodes have an obvious adhesion belt. Many large pores connect neighbouring siphons (Figs 44, 45). Median adhesion belt heights are 33–53 μm, and median supranodal siphon lengths and diameters, 163–327 μm and 95–150 μm, respectively. Medullar siphons trifurcate; they rarely branch dichotomously (Fig. 44). Median medullar siphon diameters are 85–153 μm, with median length to width ratios of 5.6–11.4.

The cortex consists of 2–3 utricle layers (Fig. 55). Peripheral utricles adhere to one another at their distal end, remaining attached after decalcification. Median peripheral utricle diameters and heights are 43–63 μm and 55–90 μm, respectively, with

median height to diameter ratios of 1.09–1.63. In surface view, peripheral utricles appear as an irregular pattern of polygons with slightly rounded corners (Fig. 56). Subperipheral utricles are not markedly inflated (Fig. 55). Secondary utricles are 42–67 μm in diameter and 52–128 μm high, with median height to diameter ratios of 1.04–2.48.

Thick, basal segments have more utricle layers than do more apical segments (Fig. 66). Basal, stipitate segments have more rigid, thick-walled and elongated utricles than segments from the central thallus region (cf. Fig. 55). The thicker cell walls are seen best in segment surface preparations (Fig. 65). Siphon fusion at nodes in the lower thallus region resembles more apical regions.

Distribution: *Halimeda incrassata* occurs in the tropical western Atlantic Ocean. It has recently been collected in Madeira, an isolated subtropical eastern Atlantic island (Wirtz & Kaufmann, 2005). The Madeiran material (vouchers H.0668 & H.0669, GENT) conforms to *H. incrassata* var. *typica* f. *gracilis* (see Børgesen, 1913), and an *rps*3 DNA barcode (Genbank accession DQ388968) confirmed its allocation to *H. incrassata*. A distribution map is shown in Fig. 71.

Halimeda melanesica *Valet (Figs 32–38, 46–48, 57, 58, 67, 68)*

Holotype: PC0021851 (PC), Lifou Island, Loyalty Islands, New Caledonia.

Description: *Halimeda melanesica* attaches to rocky substrata by means of a firm, dense mat of rhizoids (Figs 32–35) and appears to be restricted to surge-affected habitats. Individuals are known to occur in wave-affected infralittoral fringe-zones to deeper-water habitats characterized by strong swells.

Two thallus morphologies can be distinguished within this species. The first is a densely branched, compact form from shallow, wave-affected sites (Figs 32, 33, 35). The second is a laxly branched form from deeper, surge-affected sites (Fig. 34). The densely branched form has a basal zone of relatively large segments that often take the form of, or merge into, a flabellate structure from which many branches arise (Figs 32, 33). Segments are smaller towards the apices. The laxly branched form has a firm basal zone of large, rigid segments. Its upper part is more flexible and comprises smaller, thinner segments.

Centrally located segments are 3.8–5.5 mm in median length and 4.0–5.4 mm in median width, with median length to width ratios of 0.93–1.07, and median thickness ranging from 0.7–0.9 mm. Specimens of the laxly branched form contain segment morphologies toward the high end of the length and width ranges, while specimens of the densely branched form contain segments towards the low end. The segment surfaces from the central and upper thallus are generally smooth, never ruffled, and occasionally shiny. Most segments are obovate–cuneate (95%; Figs 36, 38), and elliptical and ovate segments are restricted to specimens from shallow, wave-affected sites (Fig. 37). The base is usually acute (97%; Figs 36, 38). The majority of segments are lobed (87%; Figs 36–38), predominantly (97%) trilobed and, although deep and medium lobes occur (both 23%), most lobes are shallow (54%).

Medullar siphons adhere closely at nodes, with an adhesion band in dissected nodes (Figs 46–48). Pores between parallel siphons are small (Fig. 47) or absent (Fig. 48). Adhesion belts are 25–30 μm in median height. Supranodal siphons are 356–525 μm in median height and 97–140 μm in median diameter. Medullar siphons trifurcate; they rarely branch dichotomously (Fig. 46), with median diameters of 79–108 μm, and median length to width ratios of 7.27–10.8.

The cortex consists of three utricle layers (Fig. 57). Peripheral utricles adhere to one another at their distal ends, remaining attached after decalcification. Their median heights and diameters are 40–53 μm and 40–50 μm, respectively, with median height to diameter ratios of 1.17–1.44. In surface view, peripheral utricles show a non-uniform pattern of polygons without rounded corners (Fig. 58). Subperipheral utricles are relatively slender (Fig. 57), with median secondary utricle heights and diameters of 49–92 μm and 32–45 μm, respectively, and height to diameter ratios of 0.93–1.06.

The cortex of thick, basal segments comprises 3–4 utricle layers (Fig. 68). Subperipheral utricles of the basal segments are larger and more swollen than in apical regions (cf. Fig. 57). The utricles are also more rigid and thick walled. Peripheral utricles are similar in shape and size throughout, except that they have thicker cell walls at the base (most obvious in surface view; Fig. 67). Siphon fusion at nodes in the lower thallus region is like that in more apical regions.

Distribution: *Halimeda melanesica* occurs throughout the tropical parts of the Indo-Pacific ocean basin. A distribution map is shown in Fig. 71.

Acknowledgements

HV is indebted to BOF (Ghent University, grant 011D9101), FWO-Flanders (project 3G002496 and travel grant) and the King Leopold III Fund for Nature Exploration and Conservation. ODC thanks FWO-Flanders for a postdoctoral fellowship grant. Funding for PSV and for translation of species

diagnoses was provided through the NOAA Fisheries Office of Habitat Conservation as part of the NOAA Coral Reef Conservation Program. AN is grateful for funding from the Territory of French Polynesia and the University of French Polynesia which contributed to this study. HV acknowledges Eric Coppejans (Ghent University), Wiebe Kooistra (Stazione Zoologica), and Diane and Mark Littler (Smithsonian Institution) for providing facilities and large collections of specimens, and participating in discussions about *Halimeda* taxonomy and evolution. HV thanks Ellen Cocquyt, Cathy De Maire, Christelle Van Kerckhove and Barrett Brooks for assistance in the laboratory, preparation of herbarium specimens, and help with paperwork. Claude Payri is acknowledged for facilitating field-work by HV and AN in French Polynesia and Wallis Island, and for giving access to her large collection of Pacific algae. We thank Ed Drew for sending photographs of *Halimeda* from the Great Barrier Reef, Mike Wynne and Stuart Lindsay of the University of Michigan Herbarium for sending photographs of *Halimeda* from the Marshall Islands, Bruno de Reviers and Edith Bury of the Muséum National d'Histoire Naturelle (Paris) for giving us access to the holotype of *H. melanesica*, and Sylvia Earle for making her large *Halimeda* collection available through the US National Herbarium. Latin translations of species diagnoses were provided by Mark Garland (http://www.botanicallatin.org). We thank Paul Colinvaux, Olivier Dargent, Lisette de Sénerpont-Domis, Roxie Diaz, Cristine Galanza, Llewellya Hillis, Manfred Kaufmann, Tom & Courtney Leigh, Frederik Leliaert, Lawrence Liao, Kimberly Page, Deborah Olandesca, Willem Prud'homme van Reine and Peter Wirtz for collecting specimens. Collection of the deep-water specimens of *H. kanaloana* was made possible with funds from NOAA Ocean Exploration #NA04OAR4600100 and NOAA Hawaii Undersea Research Laboratory Award #NA16RU1333.

References

Abbott, I.A. & Huisman, J.M. (2004). *Marine Green and Brown Algae of the Hawaiian Islands*. Bishop Museum Press, Honolulu, Hawaii.

Alvarez, I. & Wendel, J.F. (2003). Ribosomal ITS sequences and plant phylogenetic inference. *Mol. Phylogen. Evol.*, **29**: 417–434.

Barton, E.S. (1901). *The genus Halimeda. Siboga Expedition Monograph 60*. Brill, Leiden, The Netherlands.

Bay, L.K., Choat, J.H., Van Herwerden, L. & Robertson, D.R. (2004). High genetic diversities and complex genetic structure in an Indo-Pacific tropical reef fish (*Chlorurus sordidus*): evidence of an unstable evolutionary past? *Mar. Biol.*, **144**: 757–767.

Bernardi, G., Holbrook, S.J. & Schmitt, R.J. (2001). Gene flow at three spatial scales in a coral reef fish, the three-spot dascyllus, *Dascyllus trimaculatus*. *Mar. Biol.*, **38**: 457–465.

Børgesen, E. (1913). The marine algae of the Darish West Indies Part I. *Dansk Botanisk Arkiv*, **1**: 1–160.

Chittaro, P.M. (2004). Fish-habitat associations across multiple spatial scales. *Coral Reefs*, **23**: 235–244.

Cohen, S., Faugeron, S., Martinez, E.A., Correa, J.A., Viard, F., Destombe, C. & Valero, M. (2004). Molecular identification of two sibling species under the name *Gracilaria chilensis* (Rhodophyta, Gracilariales). *J. Phycol.*, **40**: 742–747.

Coppejans, E., Leliaert, F., Dargent, O. & De Clerck, O. (2001). The green algae (Chlorophyta) of the north coast of Papua New Guinea. *Cryptogamie Algol.*, **22**: 375–443.

Dargent, O. (1997). Etude systématique du genre *Halimeda* (Caulerpales, Bryopsidophycées), dans la zone de contact entre l'Océan Indien et l'Océan Pacifique. Masters degree thesis, Université Pierre et Marie Curie (Paris VI). Paris, France. 30 pp.

De Clerck, O., Gavio, B., Fredericq, S. & Coppejans, E. (2005). Systematics of *Grateloupia filicina* (Halymeniaceae, Rhodophyta), based on rbcL sequence analyses and morphological evidence, including the reinstatement of *G. minima* and the description of *G. capensis* spec. nov. *J. Phycol.*, **41**: 391–410.

Dragastan, O.N., Littler, D.S. & Littler, M.M. (2002). Recent vs. fossil *Halimeda* species of Angaur Island, Palau and adjacent western Pacific areas. *Acta Palaeontologica Romaniae*. Special publication no. 1. Cartea Universitara, University of Bucharest. Bucharest, Romania.

Drew, E.A. (1983). *Halimeda* biomass, growth rates and sediment generation on reefs in the central Great Barrier Reef province. *Coral Reefs*, **2**: 101–110.

Ellis, J. (1767). Extract of a letter from John Ellis, Esq. F.R.S. to Dr. Linnaeus, of Upsal F.R.S., on the animal nature of the genus of zoophytes called *Corallina*. *Philosophical Transactions*, **57**: 404–427.

Ellison, A.M., Farnsworth, E.J. & Merkt, R.E. (1999). Origins of mangrove ecosystems and the mangrove biodiversity anomaly. *Global Ecol. Biogeogr.*, **8**: 95–115.

Famà, P., Wysor, B., Kooistra, W.H.C.F. & Zuccarello, G.C. (2002). Molecular phylogeny of the genus *Caulerpa* (Caulerpales, Chlorophyta) inferred from chloroplast tufA gene. *J. Phycol.*, **38**: 1040–1050.

Freile, D., Milliman, J.D. & Hillis, L. (1995). Leeward bank margin *Halimeda* meadows and draperies and their sedimentary importance on the western Great Bahama bank slope. *Coral Reefs*, **14**: 27–33.

Geiger, D.L. (2002). Stretch coding and block coding: Two new strategies to represent questionably aligned DNA sequences. *J. Mol. Evol.*, **54**: 191–199.

Gurgel, C.F.D., Liao, L.M., Fredericq, S. & Hommersand, M.H. (2003). Systematics of *Gracilariopsis* (Gracilariales, Rhodophyta) based on rbcL sequence analyses and morphological evidence. *J. Phycol.*, **39**: 154–171.

Hillis, L. (1959). A revision of the genus *Halimeda* (order Siphonales). *Publications of the Institute of Marine Science*, **6**: 321–403.

Hillis-Colinvaux, L. (1980). Ecology and taxonomy of *Halimeda*: primary producer of coral reefs. *Adv. Mar. Biol.*, **17**: 1–327.

Kimura, M. (1980). A simple method for estimating evolutionary rate of base substitutions through comparative studies of nucleotide sequences. *J. Mol. Evol.*, **16**: 111–120.

Knowlton, N. (1993). Sibling species in the sea. *Annu. Rev. Ecol. Syst.*, **24**: 189–216.

Kooistra, W.H.C.F. & Verbruggen, H. (2005). Genetic patterns in the calcified tropical seaweeds *Halimeda opuntia*, *H. distorta*, *H. hederacea* and *H. minima* (Bryopsidales, Chlorophyta) provide insights in species boundaries and inter-oceanic dispersal. *J. Phycol.*, **41**: 177–187.

Kooistra, W.H.C.F., Calderón, M. & Hillis, L.W. (1999). Development of the extant diversity in *Halimeda* is linked to vicariant events. *Hydrobiologia*, **398**: 39–45.

Kooistra, W.H.C.F., Coppejans, E.G.G. & Payri, C. (2002). Molecular systematics, historical ecology and phylogeography of *Halimeda* (Bryopsidales). *Mol. Phylogen. Evol.*, **24**: 121–138.

Kützing, F.T. (1857). *Tabulae Phycologicae*, Vol. 7. Nordhausen, Germany.

Littler, M.M., Littler, D.S. & Lapointe, B.E. (1988). A comparison of nutrient- and light-limited photosynthesis in psammophytic versus epilithic forms of *Halimeda* (Caulerpales, Halimedaceae) from the Bahamas. *Coral Reefs*, **6**: 219–225.

Merten, S.M.J. (1971). Ecological observations of *Halimeda macroloba* Decaisne (Chlorophyta) on Guam. *Micronesica*, **7**: 27–44.

Noble, J.M. (1986). *Halimeda magnidisca* (Caulerpales, Chlorophyta), a new species from the Great Barrier Reef, Australia. *Phycologia*, **25**: 331–339.

Noble, J.M. (1987). A Taxonomic Study of the Genus *Halimeda* Lamouroux (Chlorophyta, Caulerpales) from the Heron Island Region of the Southern Great Barrier Reef, Australia. Masters degree thesis, University of Melbourne. Melbourne, Australia.

Nylander, J.A.A. (2004). *MrModeltest v2.0*. Department of Systematic Zoology, Uppsala University, Sweden.

Palumbi, S.R. (1997). Molecular biogeography of the Pacific. *Coral Reefs*, **16** (Suppl.): 47–52.

Payri, C.E. (1995). Carbonate production of some calcifying algae in a French-Polynesia coral-reef. *Bull. Soc. Géol. France*, **166**: 77–84.

Payri, C.E. & Meinesz, A. (1985). Taxonomy and distribution of the genus *Halimeda* (Chlorophyta, Caulerpales) in French Polynesia. *Proc. 5th Int. Coral Reef Congr.*, **6**: 641–648.

Payri, C., N'Yeurt, A.D.R. & Orempuller, J. (2000). *Algae of French Polynesia*. Au Vent des Iles, Tahiti, French Polynesia.

Posada, D. & Crandall, K.A. (1998). Modeltest: testing the model of DNA substitution. *Bioinformatics*, **14**: 817–818.

Provan, J., Murphy, S. & Maggs, C.A. (2004). Universal plastid primers for Chlorophyta and Rhodophyta. *Eur. J. Phycol.*, **39**: 43–50.

Ronquist, F. & Huelsenbeck, J.P. (2003). MrBayes 3: Bayesian phylogenetic inference under mixed models. *Bioinformatics*, **19**: 1572–1574.

Rossier, O. & Kulbicki, M. (2000). A comparison of fish assemblages from two types of algal beds and coral reefs in the south-west lagoon of New Caledonia. *Cybium*, **24**: 3–26.

Rotondo, G.M., Springer, V.G., Scott, G.A.J. & Schlanger, S.O. (1981). Plate movement and island integration – a possible mechanism in the formation of endemic biotas, with special reference to the Hawaiian Islands. *Systematic Zoology*, **30**: 12–21.

Sáez, A.G. & Lozano, E. (2005). Body doubles. *Nature*, **433**: 111.

Sáez, A.G., Probert, I., Geisen, M., Quinn, P., Young, J.R. & Medlin, L.K. (2003). Pseudo-cryptic speciation in coccolithophores. *Proc. Nat. Acad. Sci. USA*, **100**: 7163–7168.

South, G.R. (1992). *Contributions to a Catalogue of the Marine Algae of Fiji. 1. Halimeda (Chlorophyceae)*. Marine studies program technical report. University of the South Pacific, Suva, Fiji.

Streelman, J.T., Alfaro, M., Westneat, M.W., Bellwood, D.R. & Karl, S.A. (2002). Evolutionary history of the parrotfishes: biogeography, ecomorphology, and comparative diversity. *Evolution*, **56**: 961–971.

Swofford, D.L. (2003). *PAUP*. Phylogenetic Analysis Using Parsimony (* and other methods). Version 4*. Sinauer Associates, Sunderland, Massachusetts.

Tamura, K. & Nei, M. (1993). Estimation of the number of nucleotide substitutions in the control region of mitochondrial DNA in humans and chimpanzees. *Mol. Biol. Evol.*, **10**: 512–526.

Taylor, W.R. (1950). *Plants of Bikini and Other Northern Marshall Islands. Algae: Chlorophyceae*. Univ. of Michigan Press, Ann Arbor, MI.

Taylor, W.R. (1960). *Marine Algae of the Eastern Tropical and Subtropical Coasts of the Americas*. Univ. of Michigan Press, Ann Arbor, MI.

Tomczak, M. & Godfrey, J.S. (2003). *Regional Oceanography: An introduction*, 2nd edition. Daya Publishing House, Delhi, India.

Tseng, C.K. (1984). *Common Seaweeds of China*. Science Press, Beijing, China.

Tsuda, R.T. & Kamura, S. (1991). Floristics and geographic distribution of *Halimeda* (Chlorophyta) in the Ryukyu Islands. *Jap. J. Phycol.*, **39**: 57–76.

Valet, G. (1966). Sur une espèce rare et une nouvelle espèce d'*Halimeda* de Mélanésie. *Revue Générale de Botanique*, **73**: 680–685.

van der Strate, H.J., Boele-Bos, S.A., Olsen, J.L., van de Zande, L. & Stam, W.T. (2002). Phylogeographic studies in the tropical seaweed *Cladophoropsis membranace*a (Chlorophyta, Ulvophyceae) reveal a cryptic species complex. *J. Phycol.*, **38**: 572–582.

Verbruggen, H. & Kooistra, W.H.C.F. (2004). Morphological characterization of lineages within the calcified tropical seaweed genus *Halimeda* (Bryopsidales, Chlorophyta). *Eur. J. Phycol.*, **39**: 213–228.

Verbruggen, H., De Clerck, O., Kooistra, W.H.C.F. & Coppejans, E. (2005*a*). Molecular and morphometric data pinpoint species boundaries in *Halimeda* section *Rhipsalis* (Bryopsidales, Chlorophyta). *J. Phycol.*, **41**: 606–621.

Verbruggen, H., De Clerck, O., Schils, T., Kooistra, W.H.C.F. & Coppejans, E. (2005*b*). Evolution and phylogeography of *Halimeda* section *Halimeda* (Bryopsidales, Chlorophyta). *Mol. Phylogen. Evol.*, **37**: 789–803.

Verbruggen, H., De Clerck, O., Cocquyt, E., Kooistra, W.H.C.F. & Coppejans, E. (2005*c*). Morphometric taxonomy of siphonous green algae: a methodological study within the genus *Halimeda* (Bryopsidales). *J. Phycol.*, **41**: 126–139.

Verbruggen, H., De Clerck, O. & Coppejans, E. (2005*d*). Deviant segments hamper a morphometric approach towards *Halimeda* taxonomy. *Cryptogamie Algol.*, **26**: 259–274.

Vroom, P.S. & Smith, C.M. (2003). Reproductive features of Hawaiian *Halimeda velasquezii* (Bryopsidales, Chlorophyta), and an evolutionary assessment of reproductive characters in *Halimeda*. *Cryptogamie Algol.*, **24**: 355–370.

Wirtz, P. & Kaufmann, M. (2005). Pfennigalgen. Neu fur Madeira und den Ostatlantik: *Halimeda incrassata*. *Das Aquarium*, **431**: 48–50.

Yano, T., Kamiya, M., Arai, S. & Kawai, H. (2004). Morphological homoplasy in Japanese *Plocamium* species (Plocamiales, Rhodophyta) inferred from the Rubisco spacer sequence and intracellular acidity. *Phycologia*, **43**: 383–93.

Zharkikh, A. (1994). Estimation of evolutionary distances between nucleotide sequences. *J. Mol. Evol.*, **39**: 315–329.

Zuccarello, G.C. & West, J.A. (2003). Multiple cryptic species: molecular diversity and reproductive isolation in the *Bostrychia radicans/B. moritziana* complex (Rhodomelaceae, Rhodophyta) with focus on North American isolates. *J. Phycol.*, **39**: 948–959.

Appendix

List of studied specimens, their geographical origin and Genbank accession numbers. All specimens are in the Ghent University Herbarium (GENT) unless otherwise indicated. (HS) indicates specimen from the personal herbarium of Heather Spalding. Such specimens will be deposited in the Bishop Museum.

Species	Specimen number	Locality	Country	SSU–ITS	*tuf*A	*rpl*5–*rps*8–*inf*A	*rps*3
A. rawsonii	HV352	Drax Hall, St. Ann's Bay	Jamaica		AM049968		
F. petiolata	H.0495	Piran	Slovenia	AF416390			
H. borneensis	HV18-1	Chwaka, Zanzibar	Tanzania				AY835514
H. borneensis	HV183b	Arue, Tahiti	French Polynesia	AY786513	AM049955	AM049972	
H. cylindracea	SOC364	Socotra	Yemen	AF525546	AM049956	AM049973	
H. discoidea	SOC299	Socotra	Yemen	AF407254	AY826360	AY826376	
H. gracilis	HV317	Avatoru, Rangiroa	French Polynesia	AY786526	AM049965	AY826384	
H. heteromorpha	HEC12238	Chwaka, Zanzibar	Tanzania				
H. heteromorpha	HOD-TZ97-435	Chwaka, Zanzibar	Tanzania				
H. heteromorpha	HV22	Chwaka, Zanzibar	Tanzania				AY835531
H. heteromorpha	HEC11946	Matemwe, Zanzibar	Tanzania				
H. heteromorpha	HEC12065	Matemwe, Zanzibar	Tanzania				
H. heteromorpha	HIMS0020	La Digue	Seychelles				
H. heteromorpha	SEY313	La Digue	Seychelles				
H. heteromorpha	SEY314	La Digue	Seychelles				
H. heteromorpha	SEY326	La Digue	Seychelles				
H. heteromorpha	SEY112	Praslin	Seychelles				
H. heteromorpha	HEC6140	Bi Ya Doo	Maldives				
H. heteromorpha	HEC12568	Magala Furi	Maldives				
H. heteromorpha	L.0399613 (L)	Panjang, Berau	Indonesia				
H. heteromorpha	Snellius-II-10506	Sumba	Indonesia	AY835468			
H. heteromorpha	HV629	Olango	Philippines	AY835473			AY835537
H. heteromorpha	HV636	Olango	Philippines	AY835474			AY835538
H. heteromorpha	HEC12271	Olango	Philippines				
H. heteromorpha	PH245	Olango	Philippines				
H. heteromorpha	HV763	Tangat	Philippines	AY835475			AY835539
H. heteromorpha	PH194	Mactan	Philippines				
H. heteromorpha	PH197	Mactan	Philippines	AF407241			
H. heteromorpha	no voucher	Mactan	Philippines	AF525568			
H. heteromorpha	HOD-PH99-109	Sanga Sanga	Philippines				
H. heteromorpha	HOD-PH99-117	Sanga Sanga	Philippines				
H. heteromorpha	HOD-PH99-128	Sanga Sanga	Philippines				
H. heteromorpha	C&PvR13144	Madang	Papua New Guinea				
H. heteromorpha	C&PvR13284	Madang	Papua New Guinea				
H. heteromorpha	C&PvR13322	Madang	Papua New Guinea				
H. heteromorpha	C&PvR13398	Madang	Papua New Guinea				
H. heteromorpha	C&PvR13492	Madang	Papua New Guinea				
H. heteromorpha	C&PvR13613	Madang	Papua New Guinea				
H. heteromorpha	C&PvR13703	Madang	Papua New Guinea				
H. heteromorpha	C&PvR13860	Madang	Papua New Guinea				

H. heteromorpha	HEC4514	Madang	Papua New Guinea				
H. heteromorpha	HEC7537	Madang	Papua New Guinea				
H. heteromorpha	HEC7551	Madang	Papua New Guinea				
H. heteromorpha	HEC7589	Madang	Papua New Guinea				
H. heteromorpha	H.0016	Great Barrier Reef	Australia	AF525569			AY835529
H. heteromorpha	H.0019	Great Barrier Reef	Australia	AF525572			AY835530
H. heteromorpha	H.0022	Great Barrier Reef	Australia	AF525571			
H. heteromorpha	US209073 (US)	Moen, Chuuk (Truk)	Micronesia				
H. heteromorpha	D&ML32062 (US)	Mbike (Florida Islands)	Solomon Islands				
H. heteromorpha	D&ML24042 (US)	Dravuni	Fiji				
H. heteromorpha	D&ML26022 (US)	Dravuni	Fiji				
H. heteromorpha	D&ML54557 (US)	Dravuni	Fiji				
H. heteromorpha	D&ML26890 (US)	Great Astrolabe Reef	Fiji				
H. heteromorpha	D&ML26021 (US)	Aitutaki	Cook Islands				
H. heteromorpha	D&ML25627 (US)	Rarotonga	Cook Islands				
H. heteromorpha	D&ML25742 (US)	Rarotonga	Cook Islands				
H. heteromorpha	H.0064	Marquesas Islands	French Polynesia				
H. heteromorpha	H.0065	Marquesas Islands	French Polynesia				
H. heteromorpha	UPF097 (UPF)	Marquesas Islands	French Polynesia				
H. heteromorpha	HV104	Moorea	French Polynesia	AF525570			AY835532
H. heteromorpha	HV144	Moorea	French Polynesia	AY835471			AY835533
H. heteromorpha	HV146	Moorea	French Polynesia		AM049957	AM049977	AY835534
H. heteromorpha	HV149	Moorea	French Polynesia	AY835472			AY835535
H. heteromorpha	H.0035	Tahiti	French Polynesia	AF407242			
H. heteromorpha	H.0036	Tahiti	French Polynesia	AY835469			
H. heteromorpha	HV231	Tahiti	French Polynesia				AY835536
H. heteromorpha	UPF097 (UPF)	Tahiti	French Polynesia				
H. heteromorpha	UPF2808 (UPF)	Tahiti	French Polynesia				
H. heteromorpha	UPF2809 (UPF)	Tahiti	French Polynesia				
H. heteromorpha	UPF2815 (UPF)	Tahiti	French Polynesia				
H. heteromorpha	UPF2823 (UPF)	Tahiti	French Polynesia				
H. heteromorpha	H.0040	Rangiroa	French Polynesia	AY835470			
H. heteromorpha	H.0045	Rangiroa	French Polynesia	AF525573			
H. incrassata	H.0136	St Martin	Netherlands Antilles				
H. incrassata	H.0179	Lee Stocking	Bahamas	AF407233	AM049958	AM049975	AY835552
H. incrassata	H.0145	Florida	USA				
H. incrassata	H.0146	Florida	USA				
H. incrassata	H.0149	Florida	USA				
H. incrassata	H.0180	Florida	USA				
H. incrassata	H.0181	Florida	USA				
H. incrassata	H.0182	Florida	USA				
H. incrassata	H.0183	Florida	USA				
H. incrassata	HV978	Florida Keys	USA				
H. incrassata	H.0236	Texas	USA				
H. incrassata	HV448	Discovery Bay	Jamaica				
H. incrassata	HV899	Priory	Jamaica				

(*continued*)

Appendix. Continued

Species	Specimen number	Locality	Country	SSU–ITS	*tuf*A	*rpl*5–*rps*8–*inf*A	*rps*3
H. incrassata	HV332	St. Ann's Bay	Jamaica				
H. incrassata	HV334	St. Ann's Bay	Jamaica				
H. incrassata	H.0229	Puerto Morelos	Mexico				
H. incrassata	H.0077	Bocas del Toro	Panama				
H. incrassata	H.0079	Bocas del Toro	Panama				
H. incrassata	H.0127	Bocas del Toro	Panama				
H. incrassata	H.0188	Bocas del Toro	Panama				
H. incrassata	H.0477	Bocas del Toro	Panama				
H. incrassata	H.0027	Galeta	Panama				
H. incrassata	H.0143	Isla Grande	Panama				
H. incrassata	H.0667	Long Key	Panama				
H. incrassata	H.0132	San Andres	Panama				
H. incrassata	H.0211	San Blas	Panama				
H. incrassata	H.0248	San Blas	Panama				
H. incrassata	H.0666	San Blas	Panama				
H. kanaloana	HS-2004-157 (HS)	Kaho'olawe	Hawai'i (USA)				
H. kanaloana	HS-2004-159 (HS)	Kaho'olawe	Hawai'i (USA)				
H. kanaloana	HS-2004-161 (HS)	Kaho'olawe	Hawai'i (USA)				
H. kanaloana	BISH715565 (BISH)	Keyhole, Mau'i	Hawai'i (USA)				
H. kanaloana	HS-2004-162 (HS)	Keyhole, Mau'i	Hawai'i (USA)				
H. kanaloana	HS-2004-171 (HS)	Keyhole, Mau'i	Hawai'i (USA)				
H. kanaloana	HS-2004-173 (HS)	Keyhole, Mau'i	Hawai'i (USA)				
H. kanaloana	HS-2004-174 (HS)	Keyhole, Mau'i	Hawai'i (USA)				
H. kanaloana	HS-2004-175 (HS)	Keyhole, Mau'i	Hawai'i (USA)				
H. kanaloana	HS-2004-176 (HS)	Keyhole, Mau'i	Hawai'i (USA)				
H. kanaloana	HS-2004-177 (HS)	Keyhole, Mau'i	Hawai'i (USA)				
H. kanaloana	HS-2004-178 (HS)	Keyhole, Mau'i	Hawai'i (USA)				
H. kanaloana	H.0649	Honolua Bay, Mau'i	Hawai'i (USA)	AY835476	AM049959	AM049978	AY835540
H. kanaloana	H.0650	Honolua Bay, Mau'i	Hawai'i (USA)	AY835477			AY835541
H. kanaloana	H.0651	Honolua Bay, Mau'i	Hawai'i (USA)	AY835478			AY835542
H. kanaloana	H.0652	Honolua Bay, Mau'i	Hawai'i (USA)	AY835479			AY835543
H. kanaloana	H.0653	Honolua Bay, Mau'i	Hawai'i (USA)	AY835480			
H. kanaloana	H.0654	Honolua Bay, Mau'i	Hawai'i (USA)				
H. kanaloana	H.0655	Honolua Bay, Mau'i	Hawai'i (USA)				
H. kanaloana	H.0656	Honolua Bay, Mau'i	Hawai'i (USA)				
H. kanaloana	H.0657	Honolua Bay, Mau'i	Hawai'i (USA)				
H. kanaloana	H.0658	Honolua Bay, Mau'i	Hawai'i (USA)				
H. macroloba	HV38	Nungwi, Zanzibar	Tanzania	AY786514	AM049960	AM049979	AY835562
H. macroloba	no voucher	Zanzibar	Tanzania	AF525561			
H. macroloba	HEC12583	Zanzibar	Tanzania	AF407240			
H. macroloba	H.0157	Pangasinan	Philippines	AF525560			
H. macroloba	H.0158	Pangasinan	Philippines	AF525566			
H. macroloba	no voucher	Zamboanga	Philippines	AF525565			
H. macroloba	no voucher	Lizard Island	Australia	AF525567			

H. macroloba	H.0228	Exmouth, W Australia	Australia	AF525562			
H. macroloba	H.0060	Viti Levu	Fiji	AF525564			
H. macroloba	H.0038	Tahiti	French Polynesia	AF525563			
H. macroloba	HV206	Faaa, Tahiti	French Polynesia	AY786515			
H. melanesica	HEC8243	Diani, Kenya	Kenya				
H. melanesica	HEC5564	Mombasa	Kenya				
H. melanesica	HEC5671	Mombasa	Kenya				
H. melanesica	HEC5860	Mombasa	Kenya				
H. melanesica	HEC7216	Mombasa	Kenya				
H. melanesica	HEC6814	Tiwi	Kenya				
H. melanesica	HEC6816	Tiwi	Kenya				
H. melanesica	HEC8386	Tiwi	Kenya				
H. melanesica	US074504 (US)	Keeli-Kudah	Sri Lanka				
H. melanesica	US030312 (US)	Keeli-Kudah	Sri Lanka				
H. melanesica	Berau-03-462 (L)	Maratua, Berau	Indonesia				
H. melanesica	Snellius-II-11254	Taka Bone Rate	Indonesia				
H. melanesica	Snellius-II-11312	Taka Bone Rate	Indonesia				
H. melanesica	Snellius-II-11180	Tukang Besi	Indonesia				
H. melanesica	US013670 (US)	Bisucay	Philippines				
H. melanesica	US013672 (US)	Canipo	Philippines				
H. melanesica	US013673 (US)	Cuyo	Philippines				
H. melanesica	HV818	Dancalan, Luzon	Philippines				
H. melanesica	PH318	Dancalan, Luzon	Philippines				
H. melanesica	HV790	Dapdap, Luzon	Philippines	AY835496	AM049961	AM049974	AY835565
H. melanesica	HEC12322	Dapdap, Luzon	Philippines				
H. melanesica	PH278	Dapdap, Luzon	Philippines				
H. melanesica	PH401	Zamboanga	Philippines				
H. melanesica	PH402	Zamboanga	Philippines				
H. melanesica	PH456	Zamboanga	Philippines				
H. melanesica	PH495	Zamboanga	Philippines				
H. melanesica	PH521	Zamboanga	Philippines				
H. melanesica	PH522	Zamboanga	Philippines				
H. melanesica	HOD-PH99-42	Zamboanga	Philippines				
H. melanesica	HOD-PH99-48	Zamboanga	Philippines				
H. melanesica	HOD-PH99-54	Zamboanga	Philippines				
H. melanesica	HOD-PH99-111	Sanga Sanga	Philippines				
H. melanesica	US071055 (US)	Agat	Guam				
H. melanesica	C&PvR13761	Madang	Papua New Guinea				
H. melanesica	HEC6547	Madang	Papua New Guinea				
H. melanesica	HEC7849b	Madang	Papua New Guinea				
H. melanesica	D&ML26246 (US)	Vatilau	Solomon Islands				
H. melanesica	D&ML26249 (US)	Vatilau	Solomon Islands				
H. melanesica	PC0021851 (PC)	Lifou	New Caledonia				
H. melanesica	D&ML25466 (US)	Aitutaki	Cook Islands				
H. melanesica	H.0665	Seashell Cove	Fiji				
H. melanesica	HV217	Afaahiti, Tahiti	French Polynesia				

(*continued*)

Appendix. Continued

Species	Specimen number	Locality	Country	SSU–ITS	*tuf*A	*rpl*5–*rps*8–*inf*A	*rps*3
H. melanesica	UPF094 (UPF)	Afaahiti, Tahiti	French Polynesia				
H. melanesica	UPF2804 (UPF)	Afaahiti, Tahiti	French Polynesia				
H. melanesica	UPF2811 (UPF)	Afaahiti, Tahiti	French Polynesia				
H. melanesica	UPF2812 (UPF)	Afaahiti, Tahiti	French Polynesia				
H. melanesica	UPF2813 (UPF)	Afaahiti, Tahiti	French Polynesia				
H. melanesica	UPF2821 (UPF)	Afaahiti, Tahiti	French Polynesia				
H. melanesica	UPF2832 (UPF)	Afaahiti, Tahiti	French Polynesia				
H. melanesica	H.0061	Marquesas Islands	French Polynesia				
H. melanesica	UPF095 (UPF)	Marquesas Islands	French Polynesia				
H. micronesica	WLS420-02	Uvea Island	Wallis & Futuna	AY786518	AM049964	AM049980	
H. monile	HV344	St Ann's Bay	Jamaica				AY835572
H. monile	H.0034	Galeta	Panama		AM049962	AM049976	
H. monile	H.0228b	Puerto Morelos	Mexico	AF407234			
H. opuntia	H.0262	Tamandare	Brazil	AF525639			
H. opuntia	HV61	Cook Bay, Moorea	French Polynesia		AM049967	AM049982	
H. simulans	HV449	Discovery Bay	Jamaica	AY835511	AM049963		
H. simulans	H.0032	Galeta	Panama				AY835573
H. taenicola	HV285-1	Tiputa, Rangiroa	French Polynesia		AM049966	AY826381	
P. capitatus	H.0349	San Blas	Panama	AF416404			
P. floridanum	KZNb2241	Sodwana Bay	South Africa		AM049969		
U. flabellum	H.0415	Portobelo	Panama	AF407270			
U. orientalis	HV817	Bulusan, SW Luzon	Philippines		AM049970		
T. expeditionis	HV873	Balicasag	Philippines		AM049971		